THE DESIGN OF ELECTROCHEMICAL CELLS FOR

UTILIZATION IN NUCLEAR MAGNETIC RESONANCE INVESTIGATIONS

by

Patrick John Faustino

Submitted in Partial Fulfillment of the Requirements

for the Degree of

Master of Science

in the

Chemistry Program

_____ _June 3, 1985_
Advisor   Date

Sally M. Hotchkiss   _June 10, 1985_
Dean of the Graduate School   Date

YOUNGSTOWN STATE UNIVERSITY

June, 1985

YOUNGSTOWN STATE UNIVERSITY

Graduate School

THESIS

Submitted in Partial Fulfillment of the Requirements

For the Degree of Master of Science

TITLE   The Design of Electrochemical Cells for Utilization in Nuclear

Magnetic Resonance Investigations

PRESENTED BY   Patrick John Faustino

ACCEPTED BY THE DEPARTMENT OF CHEMISTRY

Daryl W. Whitney   _June 3, 1985_
Major Professor   Date

Howard D. Mettee   _June 3, 1985_
                                             Date

Thomas N. Dobbelstein   _June 4, 1985_
                                             Date

Sally M. Hotchkiss   _June 10, 1985_
Dean, Graduate School   Date

ABSTRACT

THE DESIGN OF ELECTROCHEMICAL CELLS FOR

UTILIZATION IN NUCLEAR MAGNETIC RESONANCE INVESTIGATIONS

Patrick John Faustino

Master of Science

Youngstown State University, 1985

The present work is concerned with the design and characterization of an electrochemical cell that can generate free radicals in concentrations that can be detected by nuclear magnetic resonance spectroscopy.

Electrochemical characterization of a cell that utilizes a stationary porous flow-through electrode made of reticulated vitreous carbon is demonstrated. The cell behavior is investigated when placed in a stirred solution provided by a spinning NMR tube.

The characterization of the electrochemical cell is done by a number of methods. Initially, resistance measurements are conducted with various surfactants to characterize the lower limit of resistance of the cell when spinning or not spinning.

The time-current characteristics of controlled potential experiments on potassium ferrocyanide are examined using different solution concentrations to determine the effective electrode surface area, diffusion layer thickness and electrolysis parameter, k, which can be used to calculate the operating efficiency of the electrochemical cell. Chronoamperometric experiments are used to

demonstrate the benefit of forced convection (increased efficiency) as a result of cell spinning.

The cell behavior is measured by cyclic voltammetry using potassium ferrocyanide as a cell standard to determine proper operation. Ascorbic acid and ninhydrin were used as test systems to indicate the potential for studies on aromatic biological compounds.

Finally, potential-step cyclic voltammetry is used to observe the cation radical of p-phenylenediamine and to determine its stability.

ACKNOWLEDGEMENTS

I extend my thanks and sincere appreciation to
Dr. Daryl W. Mincey for his patience and guidance throughout this
research. I also thank Dr. Thomas Dobbelstein and Dr. Howard Mettee
for reviewing the manuscript.

Special thanks is extended to Mr. Marc J. Popovich for his
help during the development of the first cell.

TABLE OF CONTENTS

LIST OF SYMBOLS

SYMBOL	DEFINITION	UNITS OR REFERENCE
A	Ampere	coulombs/sec
A'	Area	
C	Capacitance	
C^b	Concentration in bulk solution	
C_D	Diffuse layer capacitance	
C_H	Helmholtz layer capacitance	
C_o	Initial concentration	
C_s	Concentration on electrode surface	
CV	Cyclic voltammetry	
Do	Diffusion coefficient	
E	Potential	volts
ESR	Electron Spin Resonance	
F	Faraday's constant	96,494 coulombs
g	Gram	
i	Current density	A/cm^2
I	Current	A
k	Electrolysis parameter	sec^{-1}
L	Liter	
M	Molarity	moles per liter
mA	Milliampere	1×10^{-3} ampere
mg	Milligram	1×10^{-3} gram
mL	Milliliter	1×10^{-3} liter
ms	Millisecond	1×10^{-3} second
mV	Millivolt	1×10^{-3} volt

SYMBOL	DEFINITION	UNITS OR REFERENCE
NHE	Normal hydrogen electrode	
NMR	Nuclear magnetic resonance	
%	Percentage	
IR	Potential drop	
redox	Oxidation or Reduction	
rf	Radio frequency	
rpm	Rotations per minute	
RVC	Reticulated vitreous carbon	
S	Diffusion layer thickness	
SCE	Saturated calomel electrode	
s	Second	
t	Time	
UV-VIS	Ultraviolet-visible	
u	magnetic moment	
μ	microunits	1×10^{-6} n-units
V	Volume	

LIST OF FIGURES

LIST OF TABLES

CHAPTER I

INTRODUCTION

Recently, there has been an increased level of research into the nature and function of reaction intermediates in the human body. This inquiry has brought forth many new hypotheses that center around the role of radical reaction intermediates in the aging process or even possibly cancer.[1] But, until recently, the study of reaction intermediates has been confined to two general areas of research: one being the analysis of free radicals as a rate determining step in organic reactions by photolysis, and the second a byproduct of electrolysis in electrochemical experiments. So the question might arise, why not employ two established research techniques to explore the role of reaction intermediates in body metabolism? This question leads to a consideration of the nature of free radicals and the analytical techniques used to observe them.

It was not until 1964 that the first in situ spectrophotometric electrochemical cell was introduced.[2] This event was the initial use of spectroscopy as a probe as defined by Heineman, "to observe the consequences of electrochemical phenomena that occur in the solution undergoing electrolysis."[3] Although this first cell was quite different than those employed in this research, it is informative to describe it briefly. This provides an insight into the technical problems that exist in the assembly of a cell that can be used to generate and spectrophotometrically study reaction

intermediates. Leedy and Kuwana[2] designed optically transparent electrodes for the generation of products that can be studied by UV-VIS spectrometry. The design provided the possibility for the spectral monitoring of electroactive species during electrolysis.

Primarily, electrodes used to generate electroactive species were in the radiation pathway of the NMR instrument. Secondly, the electrodes can cause inhomogenities in the magnetic field component of the NMR. Finally, a time delay exists between the attempts to actually observe generation of the electroactive species and their detection by NMR.

Thus, the electrochemist was unable to couple the techniques together. Many complementary techniques, such as infrared and thin layer electrodes, did allow limited glimpses of free radicals with these techniques.[4,5] For example, Mark developed a cell that utilized internal reflectance.[6] These cells were positively successful, but the low signal to noise ratio of the IR technique eliminates the possibility of fast kinetic studies of transient species present at low concentrations. There is also competitive absorption of radiation by the solvent-electrolyte system. Raman spectrometry, with the application of new laser techniques, has been used sparingly but successfully.[7] Yet, in general use, Raman spectrometry is also too insensitive for low concentration levels. Fluorescence has been utilized for biochemical applications.[8] UV-VIS[9] absorption spectra have also provided some information but the broad bands encountered cause difficulty with the identification of electroactive species generated electrochemically. Figure 1 provides a schematic overview of the techniques discussed above.
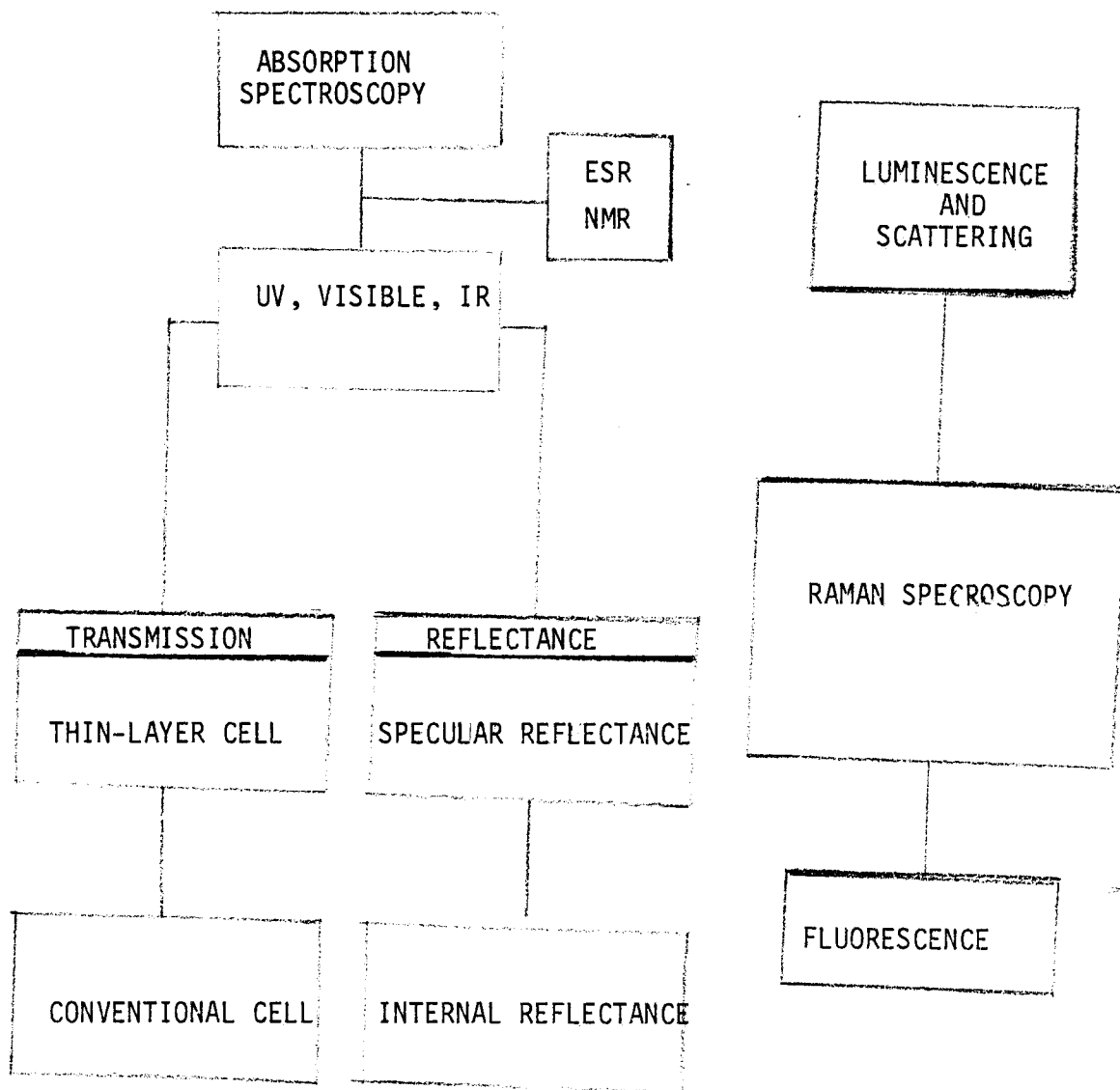
Figure 1: Spectroelectrochemical techniques

It was not until 1975 that Evans and Richards performed the first successful electrolysis within an NMR probe using an electrochemical flow cell.[10] This experiment eventually provided the impetus for the work of Mincey and Caruso, where the possible generation in situ of radical intermediates in the NMR was monitored.[11] Similar electrochemical cells have also been placed in the cavity of ESR spectrometers.[12]

Additionally, the use of NMR to study the electroactive species introduces problems. Traditionally NMR has always had a rather low sensitivity. This was too often a result of a rather weak signal that is actually produced by the NMR. It was necessary, therefore to amplify the signal and the rf background noise. The signal to noise ratio of a weak signal provided obvious difficulty with enhancement.[13] With the advent of microprocessor-based NMR systems, and the ability to perform Fourier Transform and Pulse techniques, the doors have been opened to greater quantitative opportunities.[14-16]

With the sensitivity enhancement[14-17] of the NMR and new electrochemical cell designs, it is possible to consider quantitative parameters in addition to structural and kinetic information. This extension is difficult with any of the previously mentioned complementary techniques. Therefore, the coupling of electrochemistry and NMR could provide unique opportunity to explore shortlived intermediates.

Electrochemistry

In order to appreciate the significance of cell design, it is appropriate to consider a definition of electrochemistry, and the factors that influenced this investigation with respect to mobility and generation of charged species as they relate to cell design and cell function.

Electrochemistry has sometimes been described as the study of ionic conductors, and the transfer of charge between ionic and electronic conductors. Another important description of electrochemistry is the study of the consequence of charge transfer at an interphase. This is especially significant to this endeavor since the consequence of charge transfer at the interphase affects overall cell design and function.

Electrochemistry has traditionally been divided into two parts, ionic and electrodics. Ionics deals with the properties of charged particles in the bulk of the solution. Electrodics deals with the equilibrium established and the activity occurring at the electrode surface.

Interphase

In order to understand the action of ions or charge carriers in solution, and the eventual electrogeneration of reaction intermediates, it is necessary to consider the "interphase." The interphase between solution and electrode is a region that exists between two phases (i.e., metal and electrolytic solution). This interphase is a region of transition between the metal electrode and the bulk

electrolytic solution which are separately referred to as
"phases."

It is important to distinguish between the terms interphase
and interface. Bockris states that an interface is a two dimen-
sional surface of contact of these two phases. It is an apparent
surface of contact, because when two phases come together there
is a region in which there is a continuous transition from the
properties of one phase to the properties of the other. If one
refers to this three dimensional transitional region, it is more
appropriate to use the term interphase.[18]

This study shall now consider a description of the interphase
and the problems that can occur when attempting to transfer electro-
active material to the electrode surface through the interphase.
The interphase that exists between an electrode and a solution of
electrolytes behaves like a capacitor, as first described by
Helmholtz in 1879.[19] Helmholtz stated that all excess charge is
located at the surface of the electrode, and parallel to the electrode
there exists a rigid layer or plane of oppositely charged ions. It
is possible to propose a parallel plate capacitor model to describe
the ionic double layer. Yet experimentally this proved difficult
because the double layer capacitor model tended to discharge by
electrochemical reactions taking place across the interface. This
model also took no account of the dependence of measured capacity
on the potential of the solution concentration.

These difficiencies were overcome by the Gouy-Chapman model,
which considered both potential and electrolytic concentrations.[20]

By not considering the thermal motion of molecules and the electro-
static attraction between the electrode and ions, the Helmholtz
rigid layer theory was oversimplified. Thus a more correct distri-
bution of concentration and charge was proposed.

The Gouy-Chapman model was called the diffuse double layer
model. In Chapman theory, based on the Gouy model, ions are consid-
ered point charges which, as a result of the effect of both electro-
static and thermal energies, occupy positions in the solution layer
close to the electrode but in a diffuse manner. This theory unfor-
tunately did not accurately describe matters either since deviations
were noted between the calculated and the experimental values for the
double layer capacitance. The difficulty with the Gouy-Chapman
theory is that the capacitance values were actually an order of
magnitude higher than theory in solutions of concentrations greater
than 1 M.[21] Solution concentrations apparently affected the ability
of the analyst to monitor chemical reactions effectively since his
theorical considerations of the interphase were incorrect.[22]

Eventually Stern suggested a combination of the two models.[23]
The ions represented the excess charge in the solution layer ad-
hering to the electrode like the Helmholtz planar layer and a Gouy-
Chapman diffuse double layer to describe the remainder of the inter-
phase. See Figure 2.

According to the Stern theory, the double layer is formed
because of ion absorption on the electrode resulting from electro-
static attraction. Therefore, the hydrated ions with opposite

Electrode surface

A) The Helmholtz model   x ⟶

Electrode surface

B) The Guoy-Chapman model   x ⟶

Electrode surface

C) The Stern model   x ⟶
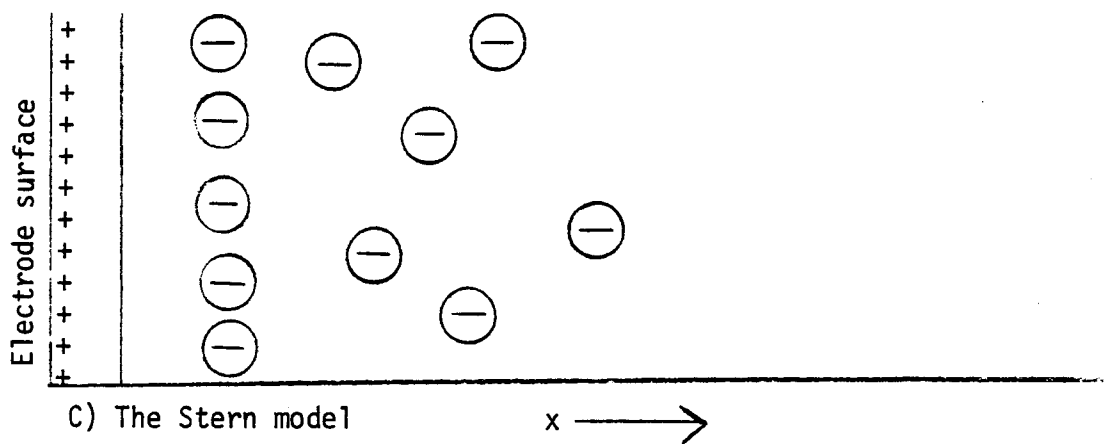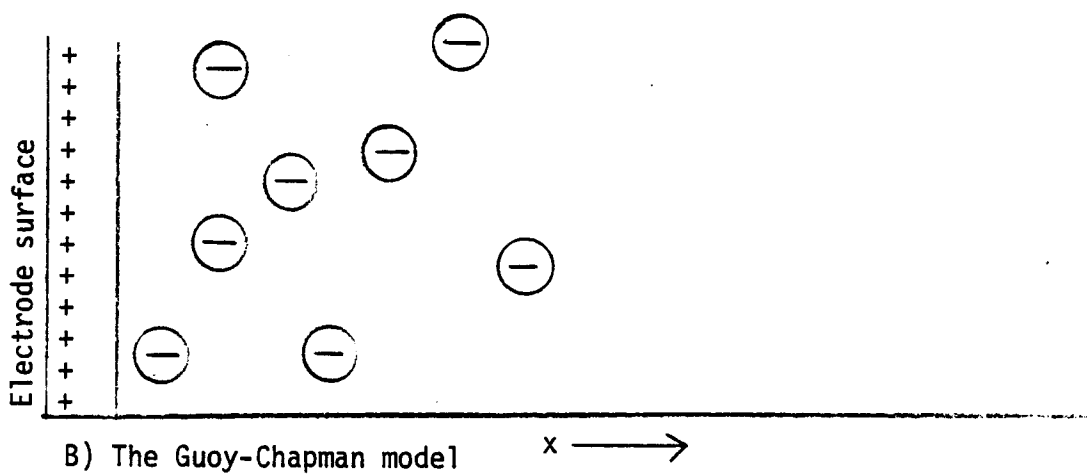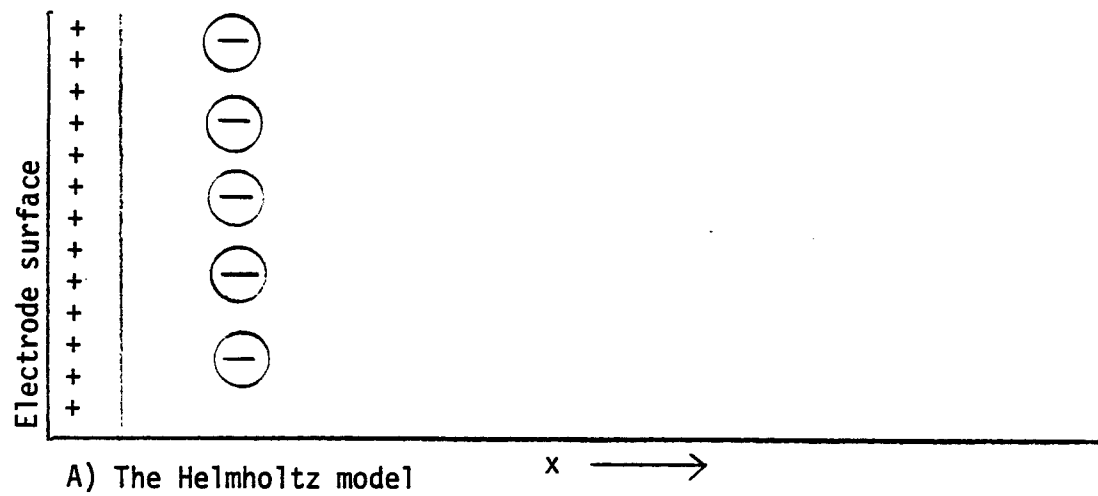
Figure 2: Interphase models

charges to the electrode surface are present in the Helmholtz layer in concentration greater than in the bulk solution and at distances from the electrode surface determined by their atomic radii and the extent of hydration. This layer's concentration is postulated to remain relatively stable. The concentration in the diffuse layer will approach the bulk concentration as a function of distance.[24]

There are two important conclusions to be drawn from the Stern model. One, a potential variation exists across two regions. A linear region associated with the charge carriers stuck to the electrode and an exponential region that corresponds to the diffuse layer affected by electrostatic forces. Two, since these layers are adjacent, Stern proposed that the Helmholtz layer and the diffuse layer be regarded as two capacitors that will act in series. Thus

$$\frac{1}{C} = \frac{1}{C_H} + \frac{1}{C_D}$$

This equation introduces the concentration problem, since the capacitance (affected by concentration) is related to these quantities.[25] The value $1/C$ is associated with those ions present in the double layer not in the bulk of the solution. These outer ions, however, have an effect on the interphasial capacitance. The concentration gradient that is present in the double layer creates an attractive environment for the ions to diffuse from the bulk solution to the double layer, as species in the double layer are in turn transported to the electrode. In spite of this shortcoming, Stern theory gives a reasonably satisfactory explanation for most interphase phenomena.

The interphasial effect on cell design is central to a
consideration of factors that determine cell efficiency. The inter-
phasial potential difference affects electrochemical reactions es-
pecially the electrogeneration of reaction intermediates such as free
radicals. This is because only small amounts of excess charge will
cause large changes in the double layer. This excess charge also
affects the electric field which is important because of the organ-
izing affects it has on ionic charge carriers. The electric field
will therefore have a stabilizing influence on the interphase and
consequently the movement of charge carriers to the electrode. The
major impact of these two potential drops is on the reaction velocity.
Therefore, it is necessary to examine the potential double layer
effects.

Interphasial Effects

Wherever there is a double layer there will be two equal, and
opposite, layers of charge and a potential difference between them.
This charge separation will produce a strong electric field. The
interphase therefore gives rise to a large accelerating force on
electric charges. The potential difference within the double layer
of the interphase is assumed by most electrochemists to be 1 Volt.[20]
The distance between the layers of charge is considered to be 0.3 nm.
Since strength is calculated as a "potential difference/distance,"
the corresponding electric field strength will be 3 X 10^9 volts/meter.
This high field strength will affect charged chemical species during
their electrochemical reactions, their reaction rates, and overall
the rate of the electrode processes.

For example, the rates of electron transfer across the inter-
faces (i.e. ionic charge carriers) are easily affected by changing
the potential of the interphase. Large changes in mobility through the
interphase can occur with only a small change of potential. When
one changes the electrode potential, the change in the electric
field strength is proportional.[26] A change in electrode potential
will change the electrode reaction rate by altering the mobility of
charged intermediates.

Electrode Reaction Rates

One of the major design factors for an efficient electro-
chemical cell is related to the rate of reaction. In this section
consideration is given to what electrode processes are, a sample
reaction that represents a redox system, and the factors that affect
the rates of reactions.

Electrode processes are chemical reactions that occur at the
interface of the electrode and the aqueous bulk solution. Electrode
reactions are heterogeneous, so the charge transfer step must occur
at the electrode interface. Since a transfer of charge occurs as a
result of these reactions, electrode processes are governed by
electron exchange.

The electrode processes, and the kinetics that control them,
are essentially the transfer of electrons from one substance to
another. A model can be used to represent the electrode reaction
as a redox system. This is done since electrochemical phenomena are
usually interpreted in terms of electron transfer during oxidation

and reduction reactions. Defining R as a reduced substance and O as an oxidized substance, the electrode reaction can be represented by,

$$O + ne \rightleftharpoons R$$
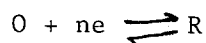
where n is the integral number of electrons exchanged. The oxidized or reduced species can be on the electrode surface or in the bulk of the solution. A consideration of the steps that occur when an oxidized species is reduced is necessary to understand the factors that govern the electrode processes. This, in turn, requires an investigation of the reaction kinetics and therefore, the electrode reaction rates.

As with many series reactions, the net rate of an electrochemical reaction is assumed to be governed by the rate of the slowest step. This in most cases will be the charge transfer step (electron exchange). An electrode reaction proceeds through the following steps,

1. The electroactive product is generated by a chemical reaction from nonelectroactive (free radical generation) substances.

2. The electroactive reactant is transported to the electrode surface.

3. The electroactive substance is absorbed on the electrode surface.

4. The electrons are transferred between the electrode and the reacting substance.

5. The product is deabsorbed from the electrode surface.

6. The product is transported to the bulk of the solution.

Bard and Faulkner summarize the above events when interpreting electrochemical kinetics as follows,

1. Mass transport from the bulk of the solution to the electrode surface.

2. Electron transfer at the electrode surface.

3. Chemical reactions that proceed or follow electron transfer.[27]

Figure 4 shows the pathway of an electrode reaction.

Mass Transport

In any discussion of interphase and electrode processes the actual transport of charge carriers to the electrode is quite important. An electrochemical cell operates on the basis of charge transfer reactions at the solution-electrode interface. If the charge transfer reaction (i.e. electron exchange) at the electrode surface is fast, the rate of the overall reaction will proceed at the rate which material is transported to the electrode surface.

This transport is accomplished in three ways: diffusion, electrostatic attraction and convection. Consideration of each of the three types of mass transport follows.

Diffusion occurs when a potential is applied at the working electrode. The electroactive species will move toward the electrode surface, react, and their concentrations in the vicinity of the electrode decrease rapidly compared to that in the bulk solution. (See Figure 5.) A concentration gradient is created as the reactants move to the electrode, and products tend to accumulate on the surface of the electrode. The electroactive species will then diffuse from the concentrated regions (bulk solution) to the now dilute region surrounding the electrode. The electron transfer reactions, that
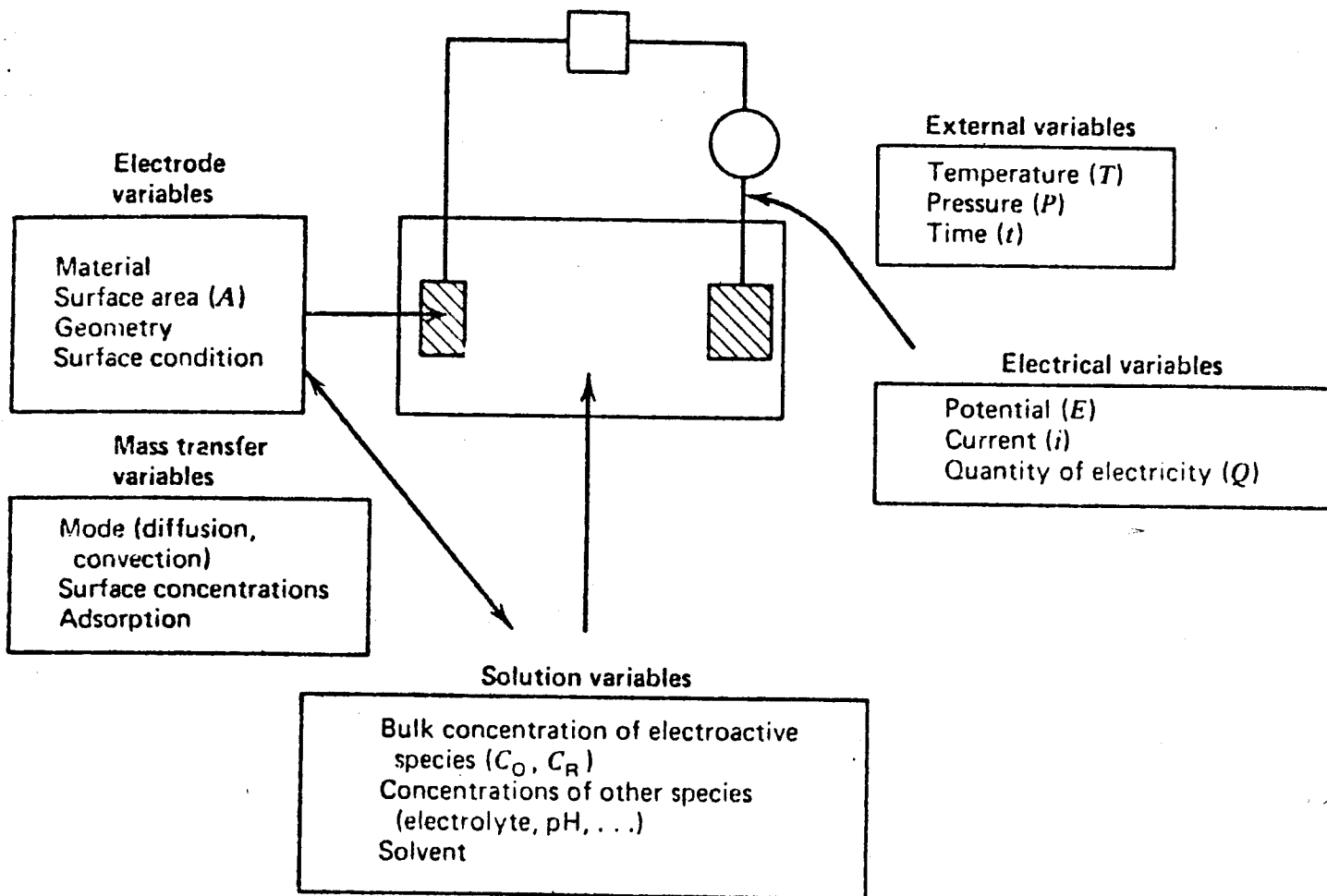
Figure 3: Variables affecting the rate of an electrode reaction.
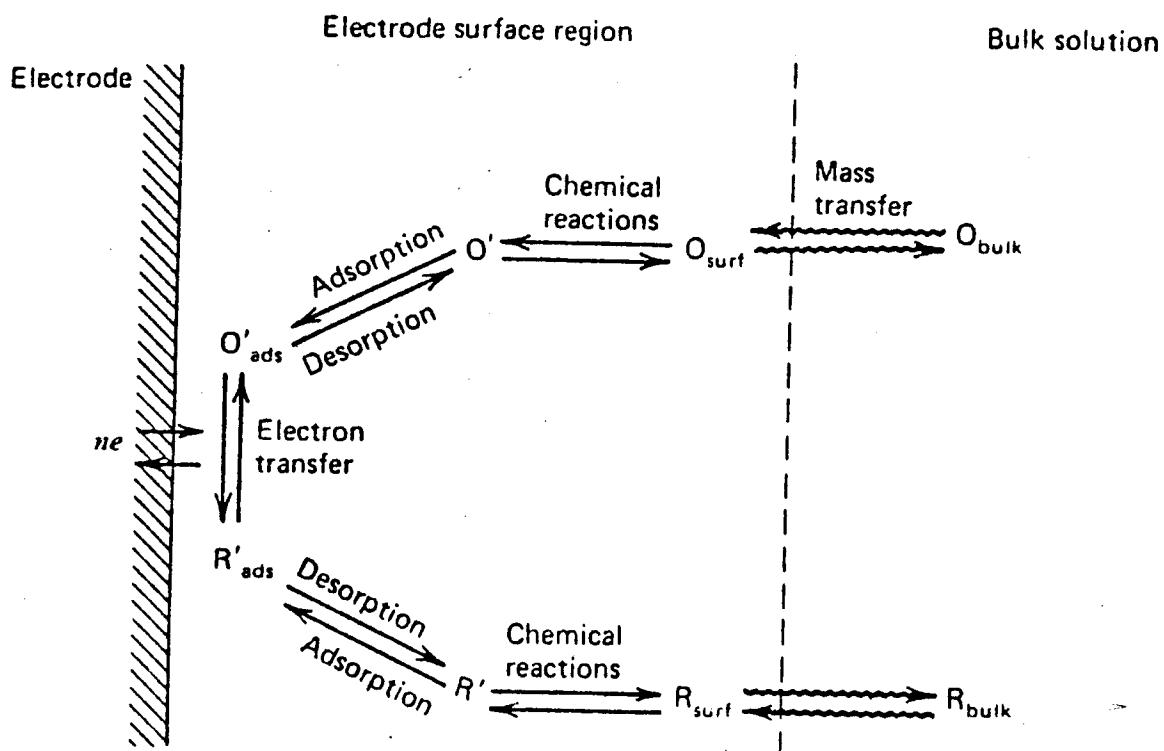
Figure 4: Pathway of a general electrode reaction.
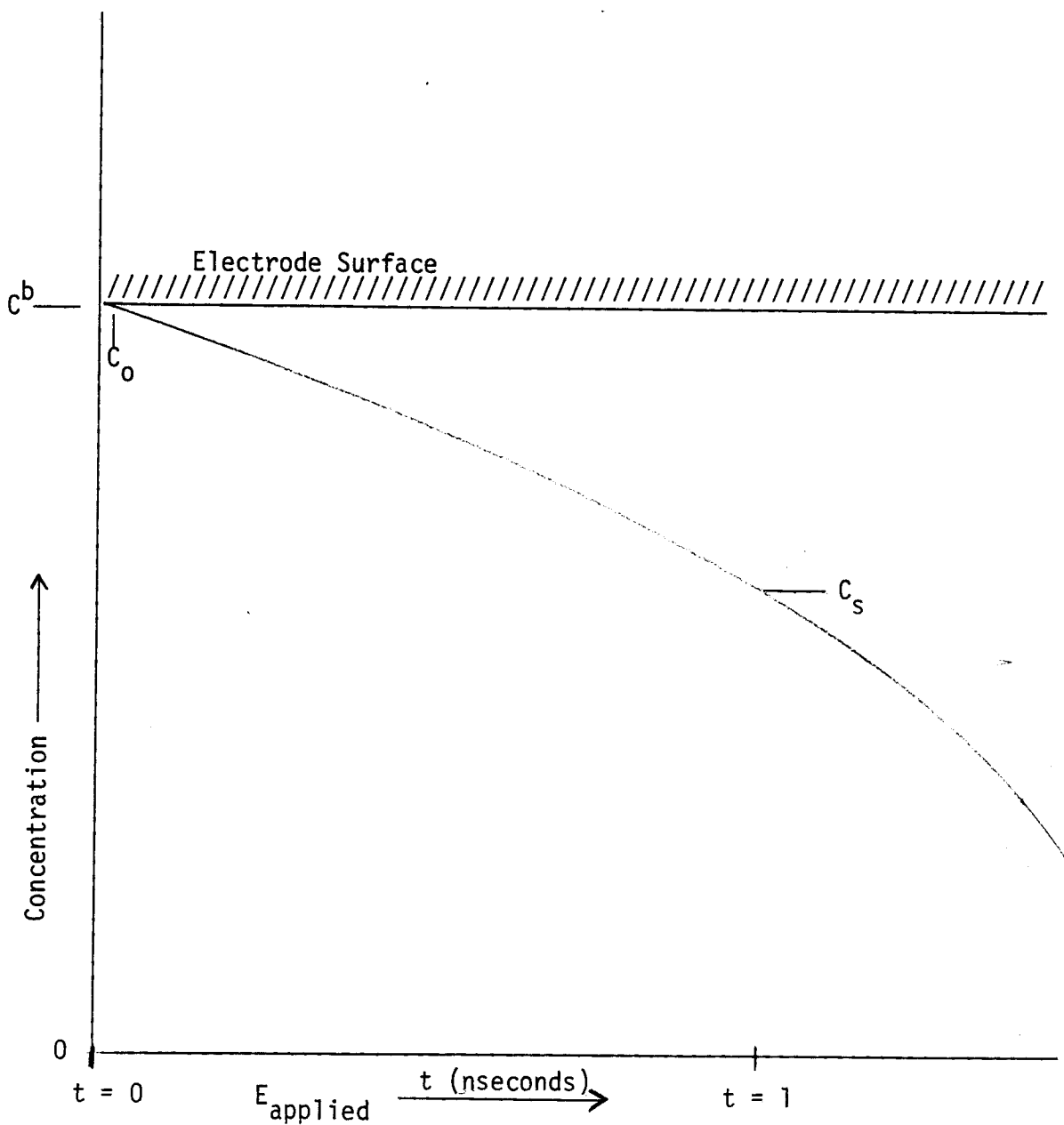
Figure 5: Concentration profile of electroactive species as a function
of time as a constant potential is applied. When no potential
is applied the concentration near the electrode will have initial
concentration $C_0 = C^b$, or the bulk concentration will be present
at the electrode surface. C_s is the concentration at time $t = 1$
indicating the period of potential being applied.

occur at the solution-electrode interface, result in a flow of current that is limited by the diffusion rate.

Electrostatic attraction can be a mass transport process. This phenomenon is known as ion migration. Ion migration is a result of a member of a redox couple, such as $FE(CN)^{3-}/Fe(CN)^{4-}$, carrying the charge in addition to maintaining the electrode process. The effect of electrostatic attraction on the electroactive species is usually minimized by adding a large excess of supporting electrolyte (usually KCl) so the electroactive species does not participate in the conduction of charge.

Convection is considered to be the thermal and mechanical motion of the molecules or ions in the solution. Convection can be avoided by minimizing external sources of heat and vibration to the electrochemical cell. Initial stirring of the solution should lead to uniform concentration to the diffusion layer or interphase.

Usually every effort is made to eliminate convection and electrostatic attraction so only diffusion is responsible for the transfer of the reactant to the surface of the electrode. This means that the transfer of electroactive species to the surface of the electrode will occur by diffusion across the solution layer that adheres directly to the electrode. Diffusion is a slow process of migration from a concentrated to less concentration region and in many cases is the rate determining step.

A simple mathematical description of diffusion is necessary to show that mass transfer takes place by a process of linear diffusion. The equations derived provide a basis for considering the efficiency

of an electrochemical cell during electrolysis. This mathematical description will account for the limiting current, or diffusion limiting current, when a steady state is obtained.

When an electrochemical current leads to the consumption of ions at the electrode, the concentration of these ions will decrease in the vicinity of the electrode surface, thereby increasing the concentration difference between the diffusion layer and the bulk solution. This results in the increase in the concentration gradient in the diffusion layer. Therefore, diffusion will occur, resulting in a decrease of the concentration gradient in the diffusion layer. Diffusion increases until the number of ions reaching the electrode by diffusion equals those consumed in the electrode process. Thus, a steady state is reached in which the current density $((A/cm^2))$ is determined by the rate of diffusion to 1 cm^2 of the surface. The current density is referred to as the "diffusion current."[28]

According to Adams, if electrolysis is carried out at constant potential, three experimental facts are noted: one is that the current is proportional to the concentration of the electroactive species in the culk solution, C_o; secondly is that the current is proportional to the area of the electrode, and third is that the current decreases with time of electrolysis.[29] A mathematical time-current relationship will be derived using linear diffusion theory, and the final result will be compared to the above experimental facts.

The number of moles of a substance "0" which diffuse past a given cross-sectional area of (cm^2) in time dt is proportional to the

concentration gradient of the diffusing species

$$\frac{dN}{dt} = KA \frac{\partial C}{\partial x}o \tag{1}$$

When the proportionality constant K is identified as the diffusion coefficient, D_o; Fick's First Law is obtained.

$$\frac{dN}{dt} = D_o A \frac{\partial C}{\partial x}o \tag{2}$$

A useful modification of this equation is obtained if it is put on a unit area basis as,

$$\frac{dN}{A\ dt} = D_o \frac{\partial C}{\partial x}o \tag{3}$$

Equation (3) defines the "flux" of material to be the number of moles diffusing per unit time through unit area. The flux is most frequently given the symbol q (or M); thus

$$q = \frac{dN}{A\ dt} = D_o \frac{\partial C}{\partial x}o \tag{4}$$

If one considers electrolysis over a period of time, it is evident that C_o, and hence C_o/dx, must decrease with time since C_o as both a function of distance from the electrode and time. In this connection, C_o should be written as C_o (x,t).

Now, the change in C_o with time between two planes at distances x and x + dx from the electrode surface (x = 0), is clearly the difference between the number of moles of O entering the plane x + dx and leaving at plane x, if the process is considered on a unit area of flux basis. Thus,

$$\frac{\partial C}{\partial t}o = \frac{q(x + dx) - q(x)}{dx} \tag{5}$$

The right side of equation (5) can be identified with dq/dx as dx approaches 0, thus:

$$\frac{\partial C}{\partial t}_o = \frac{\partial q}{\partial x} \qquad (6)$$

But the flux already has been given by equation (4) as,

$$q = D_o \frac{\partial C}{\partial x}_o$$

Thus,

$$\frac{\partial q}{\partial x} = D_o \frac{\partial^2 C}{\partial x^2}_o \qquad (7)$$

Substituting for dq/dx from equation (6) gives,

$$\frac{\partial C}{\partial t}_o = D_o \frac{\partial^2 C}{\partial x^2}_o \qquad (8)$$

This, is Fick's Second Law, the fundamental equation for linear diffusion. From Fick's Second Law it can follow that,

$$\frac{\partial C}{\partial x}_o = \text{constant} \qquad (9)$$

Therefore, in the steady state, the concentration gradient is constant throughout the diffusion layer. Here the concentration of ions maintaining the electrode is C_s at the surface and C_o in the bulk of the solution, the concentration in the diffusion layer is, where s is the length of the diffusion layer,

$$\frac{\partial C}{\partial x} = \frac{C_o - C_s}{S} \qquad (10)$$

The current provided by steady state diffusion is,

$$i = zFD_o\left(\frac{C_o - C_s}{S}\right) \qquad (11)$$

The steady state ion concentration in the vicinity of the surface is a function of the current density. If the ion concentration is low, then ions are consumed very slowly, and C_s barely differs from C_o. With increasing current density, C_s is gradually decreased and will become almost zero with respect to C_o. This corresponds to the maximum of the diffusion current or the limiting diffusion current. The limiting diffusion current may be represented as,

$$i^o_{lim} = \frac{zFD_o C_o}{s^o} \qquad (12)$$

Therefore, the limiting diffusion current is proportional to the bulk concentration of the ion which maintains the electrode process, and inversely proportion to the thickness of the diffusion layer.[30] This concentration dependence is the basis of experimental electrochemistry as it applies to potential-current analysis of redox system and its application to the analysis of electrochemical cell operation.

According to the method of Adams, equation (12) can be rewritten to give,

$$i = \frac{nFD_o C_o A'}{3.14^{1/2} t^{1/2}} \qquad (13)$$

The units for equations (13-15) are:

i = current in amperes

F = coulombs

n = number of electrons involved in the overall process

A = area in cm^2

D_o = diffusion coefficient in cm^2/sec

C_o = bulk concentration in moles/ml

t = time in seconds

this equation may be solved for A',

$$A' = \frac{(it^{1/2})\, 3.14^{1/2}}{nFD_o^{1/2}\, C_o} \qquad (14)$$

Equation (14) enables an analyst to determine the electrochemical area of an electrode, provided that n and D_o are known. Solving for D_o, the diffusion coefficient may be determined.

$$D_o = \frac{it^{1/2}\, 3.14^{1/2}}{nFA'\, C_o}^2 \qquad (15)$$

Different forms of the above equations will be used on this work to determine cell efficiency, electrode geometry, limiting current data.

Potential Drop

A second aspect of the electrode surface–interphase problem is the IR drop, or the potential drop, between the cell electrodes during current flow. The impact of this factor is as important as electrode reaction rates and mass transport to the overall problem of proper cell design. But it is quite different because it is essentially independent of the kinetics and demands a critical analysis of electrode geometry.

When the potential in an electrochemical cell is scanned positive-to-negative, a current is generated between working and the auxiliary electrodes when a redox couple is present in solution. A potential drop, or voltage drop, occurs when a current, I, passes through an electrochemical cell of resistance, R, and the "ohmic potential drop" is given by IR. This IR drop, due to internal cell resistance, creates two problems for cell design. First, the

potential drop can limit the current that can pass through the cell. Secondly, the IR drop can increase the applied potential necessary for a redox system to react, and thereby decrease the efficiency of the cell.

There are several factors that directly affect the IR drop such as high current, high solution resistance and/or fast potential change by the potentiostat scan rate. Each of these factors can be reduced by appropriate solvent systems or potentiostatic adjustments. Yet there still remains a residual IR drop. The conditions that cause IR drop, and what can be done to minimize it, need to be considered.

Current can be easily measured at the counter, or auxiliary, electrode. But unfortunately the measured potential of the working electrode is always subject to error because the reference electrode used to measure potential cannot measure at a point directly on the solution side of the interphase. The nonzero distance between these points means that current flowing through the cell between the ideal and actual measuring points is subject to a potential drop that contributes to the potential measured for the working electrode vs. the reference electrode.

There are many ways to compensate for the IR drop in the three-electrode (working, reference and counter) configuration. To adjust for the resistance of the solution, the reference electrode is placed as near as possible to the working electrode so that the measured potential at the working electrode can be monitored as closely as possible. A uniform current distribution at the working

electrode is also important, since this permits efficient monitoring by the reference electrode. This can be accomplished by employing a mercury pool, as was done in the first cell or a symmetrical electrode like that of the second electrochemical cell. Great care must be paid to electrode geometries. A non-symmetric environment around the working electrode can create inconsistent currents and nonsymmetrical potential fields in the interphase. Electrode geometry, and its relationship to cell-potentiostat systems, are extensively covered in the literature.[31-33] Other strategies of cell design have been used to minimize IR drop.[34,35]

Cell Design

A primary requirement of each cell was that controlled-potential electrolysis experiments could be conducted in a spinning NMR tube. Baizer has noted that a number of problems must be considered when designing a cell for general electrolysis – such as potential distribution at the working electrode, position of the reference electrode, position and need for a diaphragm, ohmic resistance, and mass and heat transfer.[36] Even though some of these topics have been covered, the specific geometry and cell arrangements need to be discussed in greater detail.

Potential distribution is important because the potential gradient should be the same over the entire electrode surface, so that a uniform current density distribution is obtained. This can be accomplished in two ways. Concentric or cylindrical electrodes or plane electrodes that are equal in size and parallel to each other

can be used. Unfortunately with plane parallel electrodes the effective surface area of one side of each of the electrodes is used. This is because only the electrode areas facing each other carry the current. In the former arrangement, a cylindrical working electrode may be placed between the auxiliary and reference electrodes. This concept can be taken one step further, as in both cell designs of this work.

In cell one, the working electrode is a cylindrical graphite frit that is immersed in a mercury pool. The reference electrode is concentrically placed in the auxiliary electrode. The second cell has a cylindrical working electrode that is placed concentrically inside a cylindrical auxiliary electrode, and the reference electrode is in turn concentrically placed inside working electrode.

The position of the reference electrode is also quite important in the design of electrochemical cells. Harrar and Shain have shown both theoretically and experimentally that a uniform potential distribution is only possible with concentric electrodes.[37] They also note that when the potential distribution is known only approximately, the best approach is to place the reference electrode as close to the working electrode as possible on a line of minimum distance between the working and auxiliary electrodes.

When the reference electrode is placed in front of the working electrode (usual arrangement), it has to be kept at a distance more than twice the outer diameter of the working electrode from the surface to avoid disturbing the equipotential lines. If this is not

done, considerable resistance error is produced. Placing the
reference electrode closer to the working electrode will distort
the lines of current at their point of control, causing most of
the electrode surface to be at a different potential than is
actually measured. This distorted current is especially important
since it may affect the nature of the chemical reaction itself
(i.e. fast reactions that generate free radicals). A glass frit,
such as the one used in our second design, can isolate the refer-
ence and auxiliary electrodes and reduce the IR drop, thereby
minimizing any current distortion.

The position and need for a diaphragm is important when an
electrochemical reaction produces products at the auxiliary elec-
trode that interfere with the electrode reaction at the working
electrode. A divided cell can, as noted above, also reduce the
IR drop and promote uniform current lines. (This was used in our
second cell design.)

An ideally effective electrochemical cell design should have
a spherical working electrode surrounded by a concentric auxiliary
electrode, and a spherical reference electrode that is surrounded
by the working electrode. Spherical electrodes have been used
but the hydrodynamic conditions have not yet been worked out.

Three-Electrode Cell Configuration

Since both cell designs in this work utilize the three-
electrode configuration, it is useful to consider the design and
function of a simple three-electrode cell.

A potential is applied to the working electrode. This potential is known with respect to a reference electrode. The reference electrode is often a standard calomel electrode (SCE) or a silver/silver chloride (SSC) electrode. When a substance is oxidized or reduced at a working electrode that has a fixed potential, current is produced at the working electrode and passed between the working electrode and the auxiliary electrode. Essentially the auxiliary electrode provides a place for the opposite chemical reaction to take place than that taking place at the working electrode.

The potential of the working electrode is monitored by the reference electrode, which should be in close proximity to the working electrode to minimize the potential drop. The reason that the potential is so critical is that an incorrect potential or potential lag can give incorrect current response.

The benefit of a three-electrode configuration over a two-electrode cell is the ability to ignore the current drain between the working electrode and the auxiliary electrode. The reference electrode draws nearly zero current and is stable, thereby not perturbing the working electrode potential though the auxiliary electrode potential may vary wildly.

Electrode Material

The search for an appropriate electrode material is often a difficult problem in electrochemistry. The task of finding a material that has a large potential "window" in aqueous systems, is chemically, inert, and is adaptable to various scan rates and

experimental conditions is solved by choosing reticulated Vitreous Carbon (RVC).

RVC is an electrically conductive material that is highly resistant to chemical attack. It has self-supporting three dimensional structure with a high void volume. Unlike glassy carbon, RVC is a porous material with a very low resistance to fluid flow and an extremely large surface area.

Overall RVC ideally meets many of the requirements for the present problem. RVC has an extremely low cost say relative to platinum. RVC has a useful potential range in aqueous systems of 1.2 to -1.0 Volts versus a SCE at a pH of 7.0. This large potential window is due to larger overpotentials for hydrogen and oxygen.

RVC has an increased reversibility for many redox couples and reactions that will involve electron and proton transfer. The high void volume promotes efficient circulation of fluid inside the electrode volume. This promotes very high conversion rates for flow-through systems and a high analytical signal. The high analytical signal is also a result of the large surface area of the electrode and is necessary to generate unstable radicals in high concentrations that can be seen in the NMR. But, most important is the fact that RVC is resistant to chemical attack. It does not react with strong oxidizing or reducing agents sometimes present in redox systems.

Cyclic Voltammetry

Before one can place the electrochemical cell into the NMR spectrometer it is necessary to see if the cell design will actually

function as intended. A powerful technique for this evaluation is cyclic voltammetry.[38] Since oxidation and reduction potentials are highly specific for many redox systems, appropriate electrode geometry can be investigated as well as overall cell function.

Cyclic voltammetry is essentially an extension of the voltammetric technique. A simple explanation of the experimental technique will provide the necessary background to appreciate cell function and design parameters in the experimental section.

Initially a solution of a known compound such as $K_3Fe(CN)_6$ or 9, 10 diphenylanthracene is placed into the electrochemical cell and the potential of the cell is scanned at a known scan rate to determine the oxidation and reduction potentials for the particular compound. The cyclic voltammograms produced will provide information about the efficiency of the cell as well as the ability to investigate the existence of reaction intermediates. A voltammogram is a plot of current vs. potential response of the electrochemical cell. A more extensive study of cyclic voltammetry and its relationship to cell geometry and radical existence is considered in the literature.[39-40]

Another important aspect of cyclic voltammetry to this investigation is the ability to investigate the stability of reaction intermediates or free radicals that form during electrolysis.[41] It has the further advantage of indicating the time lag that is allowable between the electrochemical generation and the NMR detection of reaction intermediates.

Cyclic voltammetry is a transient technique in which the potential supplied to the working electrode by the potentiostat is varied in a cyclic fashion. There is a linear increase in potential with time in either direction, followed by a reversal of the scanning direction and a linear decrease in potential at the same scan rate. An example of this waveform is seen in figure 6.

This waveform is known as an isosceles triangle and allows the investigator to scan the potential of the working electrode in the cathodic direction (negative, vs. ref. electrode) and observe peaks due to the reduction of a chemical species in the electrochemical cell. The potential can then be scanned in the anodic direction and peaks due to the oxidation of a chemical species can be observed. Figure 7 shows a classical, ideal, reversible, cyclic voltammogram that follows the above discussion. Note that in an electrolytic cell, reduction will occur at the cathode.

In conclusion, cyclic voltammetry provides a powerful technique for considering proper cell function and cell geometry. It can also provide information about the approximate number of electrons exchanged at each peak, as well as the reversibility of certain chemical systems. But the most important facility of cyclic voltammetry is the ability to prove the existence of unstable radicals or intermediates and estimate their lifetimes.

The NMR Experiment

Many nuclei act as charged spinning bodies and will produce, because of their spin, a magnetic moment along their axis of rotation.
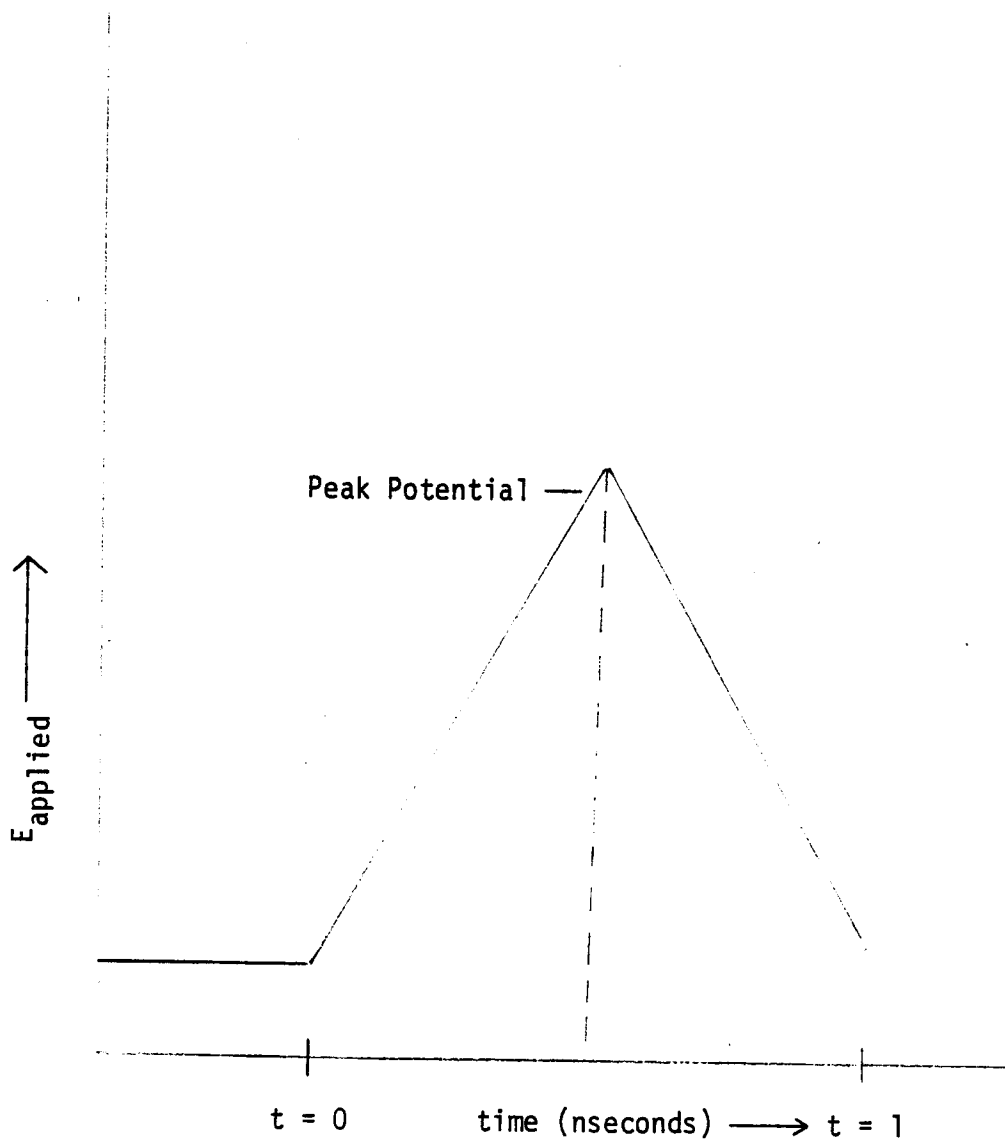
Figure 6: The applied potential waveform known as the isosceles triangle. Represented above between t = 0 and t = 1 is one triangular sweep unit.
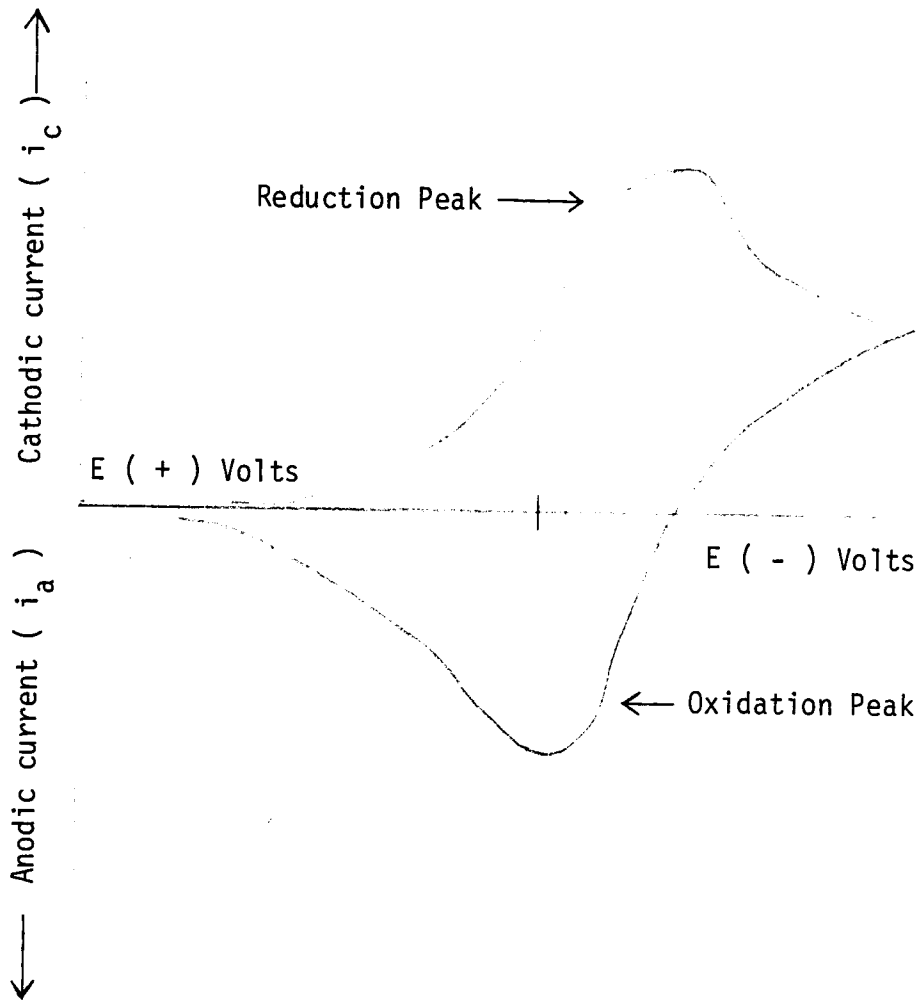
Figure 7: A classic ideal reversible cyclic voltamograms. This diagram,which is also known as a dove, is a plot of current vs. potential.

When these spinning nuclei are placed in a uniform magnetic field, they will line up with the field or against it (if they are protons), creating what is called the nuclear Zeeman splitting, or a splitting of nuclear energy levels. This splitting is similar to the splitting of electronic levels, or Zeeman effect, which is where it gets its name.

The NMR experiment induces transitions between the nuclear Zeeman levels. To produce these transitions, an alternating magnetic field is placed perpendicular to the applied magnetic field in a way that its frequency can be changed easily. When the frequency of the applied magnetic field corresponds to the energy difference between the Zeeman levels, an absorption of energy occurs and produces transitions from one nuclear energy level to the other.

Mathematically, the NMR experiment can be considered using classical mechanics. For a spin of 1/2, the possible orientations, in terms of the nuclear spin quantum number are $m = 1/2$ and $m = -1/2$, corresponding to alignment with or opposed to B_o. The interaction between the magnetic moment, μ, and B_o results in a torque acting on μ, which tends to tip u toward B_o, due to the nuclear spinning. This torque causes u to precess about the magnetic field B_o, similar to the way a gyroscope will precess about the earth's magnetic field. The presessional frequency of u about B_o is given by the Larmor equation,

$$v_o = \frac{y}{2\pi} B_o \qquad (16)$$

where v_o is the precessional frequency in cycles/sec. Thus, the precessional frequency is dependent on both B_o and y and will be different for each particular nucleus.

When a second, smaller magnetic field B_1 is applied in the x - y plane, and rotating in the same direction as μ, interactions between B_1 and μ occur. As long as B_1 is rotating at some frequency v other than the Larmor frequency v_o, the effect of B_1 on μ will result in slight oscillations of the angle between B_o and u. When B_1 is rotating at a frequency $v = v_o$, μ will feel the effects of both B_o and B_1 simultaneously, and will exhibit large oscillations in the angle between μ and B_o, and the direction of μ with respect to B_o changes. Energy is absorbed by the nucleus and the magnetic moment μ is said to have "flipped" from one orientation in the magnetic field to the other. The absorption of energy when $v = v_o$ is measured on the NMR experiment. The "chemical shift" is based on the frequency at which this absorption occurs.

NMR and Free Radicals

NMR is ideally suited to investigate free radical systems, which are molecules with at least one unpaired electron, for two reasons. Chemical species with unpaired electrons are paramagnetic. This is very important since paramagnetic species produce characteristic chemical shifts which are not many times larger than ordinary shifts seen in dimagnetic molecules.

The unpaired electron on paramagnetic species provides a very efficient relaxation mechanism. Also since relaxation processes are very sensitive to changes in environment when free radicals are produced, the resultant environmental change is readily discovered. The fundamental problem is to produce free radicals in concentrations sufficient to provide a detectable NMR signal.

CHAPTER II

STATEMENT OF PROBLEM

The primary goal of this research was to design electro-
chemical cells which could be used to control potential electroly-
sis experiments efficiently when placed in a spinning NMR tube. It
was desired to construct an electrochemical cell that could be used
to perform such experiments while simultaneously using NMR to ob-
serve transient electrochemical phenomena such as reaction inter-
mediates.

The design of the electrodes should be spherical, or cylin-
drical, and concentric to promote uniform current distribution and
efficient mass transport of electroactive species to each electrode
surface. The electrode geometry and cell design should minimize
potential drop and eliminate asymmetrical potential fields that
would disturb efficient electrolysis.

The cell should have an electrode material that has a large
potential window in aqueous systems. This electrode material should
be chemically inert and experimentally adaptable to various environ-
mental conditions such as extremes in pH, application of large
potentials, and varying scan rates.

The cell should have an electrode with flow through capabili-
ties with a high void volume that would promote efficient circulation
of fluid inside the electrode. It should have a large effective
surface area to generate transient electroactive species such as
reaction intermediates (i.e. relatively unstable free radicals) in

concentrations great enough to be detected by the NMR, yet generated from very small solution volumes and proportionally smaller electroactive material as would be found in aqueous biochemical systems of interest.

CHAPTER III

MATERIALS AND APPARATUS

Materials

All chemicals used in this research were of analytical
reagent quality.

Cell I Material Location and Design

The initial cell design used many different types of mater-
ials. We shall refer to Figure 8 to identify the various materials
and their location and elucidate cell design. At the top of Figure
8 is a 19/38 glass pyrex fitting which is internally fitted with a
19/38 pyrex glass stopper. This glass stopper has been modified
to concentrically allow glass tube A (.221 cm OD) of 13.97 centi-
meters in length, of which 1.90 cm is internally epoxied in the
19/38 stopper that has been drilled to accommodate tube A. The
entire tube A is then placed into a standard NMR tube (.518 cm OD)
thats sits in the NMR spinner assembly. The NMR tube or tube B is
epoxied at the top to a plastic cylinder (1.48 cm OD) that allows
tube B to sit in the spinner assembly. At the bottom of tube B is
a graphite cylinder that extends 1.1 centimeters. This graphite
cylinder is held in place by standard heat shrink at the bottom of
tube B. A second NMR tube like tube B with a length of 16.51 cm
extends down. At the top of this second tube is a graphite cup

Reference electrode wire lead

Auxiliary electrode wire lead

19/38 fitted glass fitting

Pyrex 19/38 glass fitting

Air holes for spinning

Plastic epoxied NMR tube holder

Standard NMR spinner assembly

Glass tube A

NMR tube B

Concentrically placed reference assembly

Auxiliary electrode

Working electrode

Hg pool

Hg pool cup
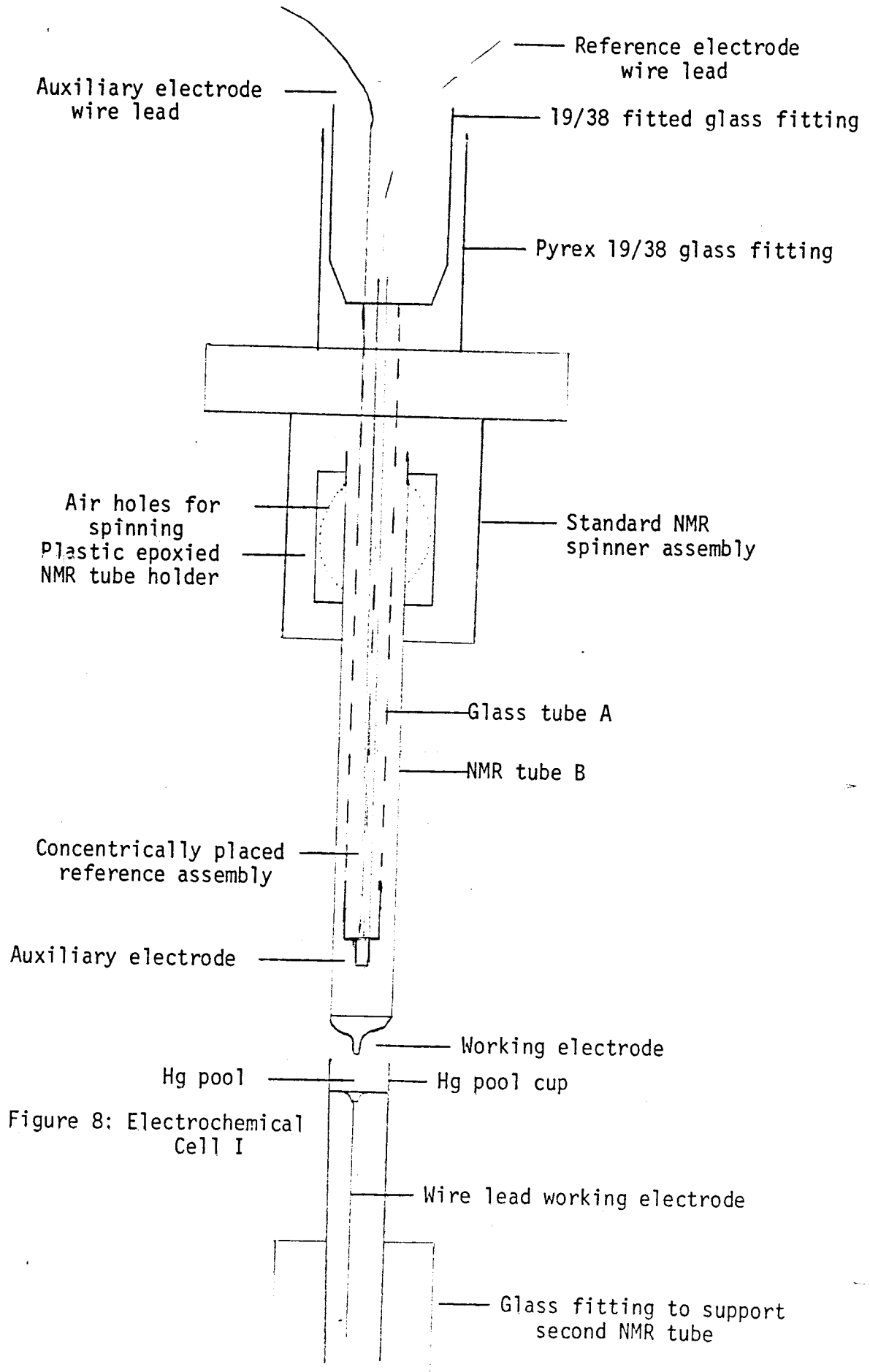
Figure 8: Electrochemical Cell I

Wire lead working electrode

Glass fitting to support second NMR tube

(.538 cm OD) which contains a mercury pool that is the contact point for the working electrode. Inside the tube is a wire lead that is silver epoxied to the graphite cup and that extends down the NMR and out the bottom to provide a potential contact for the potentiostat. The graphite cup is held in place by standard heat shrink. The reference electrode is located inside tube A. The reference electrode is a Ag/AgCl wire that is immersed in a 4M solution of KCl and saturated silver ion. The auxiliary electrode is a graphite cylinder that is located at the bottom of tube A. The auxiliary electrode extends up along tube A 10 cm. The Ag wire auxiliary electrode lead is isolated from the solution in tube B by heat shrink that extends up tube A 9.52 centimeters.

<div align="center">Cell II Material Location and Design</div>

The second cell was quite different from the first both in materials used and cell design. Figure 9 identifies the various materials and their location as assembled in the second cell. At the top of Figure 9 is a glass tube A (.312 cm OD) that extends 13.97 centimeters in length. At the base of this glass tube A is a vycor plug of the same diameter with a length of .635 cm. The Tube A assembly is placed approximately 1.75 cm, concentrically, inside electrode material called reticulated vitreous carbon (.665 cm OD), of length 3.17 centimeters. The electrode material of RVC and the glass tube A are held together by silver epoxy. Tube A is then placed inside tube B which is a standard NMR tube (1.00 cm OD) of a length of 10.8 centimeters. At the base of tube B is a porous

Reference electrode lead

Working electrode lead

Epoxied NMR tube holder

NMR Spinner assembly

Air holes

Auxiliary electrode lead

tube B

tube A

Ag/AgCl wire

Heat Shrink

Silver Epoxy

1.0M KCl

RVC Working Electrode Internal Cavity

Vycor Plug

Glass Frit

RVC Auxiliary Electrode
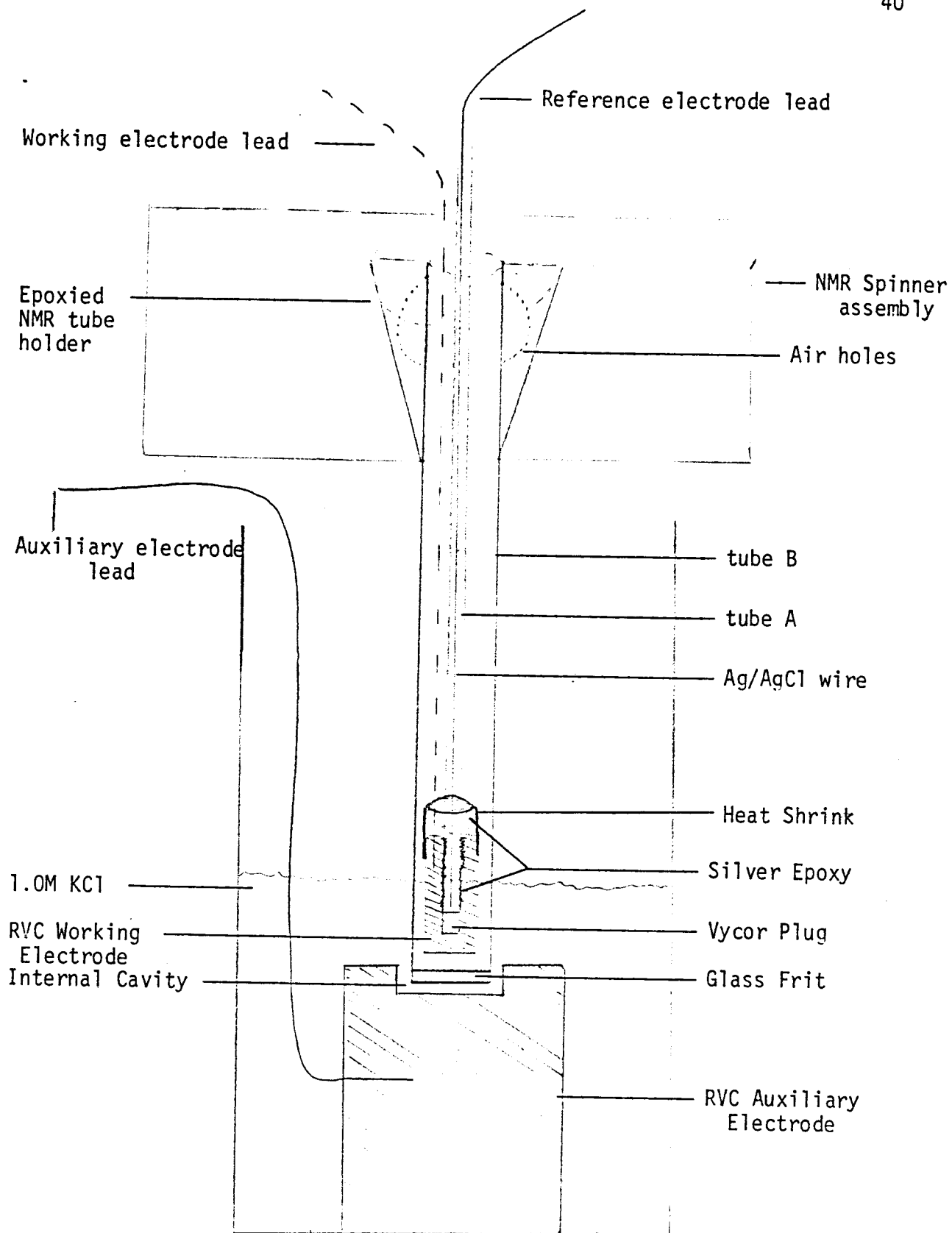
Figure 9: Electrochemical Cell II

glass frit of the same diameter, and a length of .289 cm, that is held on to tube B by standard heat shrink. At the top of Tube B is a plastic cylinder (1.69 cm OD) epoxied to Tube B so that Tube B can sit in an appropriate NMR spinner assembly. Tube B is then lowered into the internal cavity of the RVC auxiliary electrode (1.25 cm OD). The internal cavity depth of the auxiliary electrode is approximately .40 centimeters. The working electrode lead is copper wire (24 gauge) that is silver epoxied to the reticulated vitreous carbon after being placed 1.25 centimeters into the RVC. The RVC—silver epoxied interface, and each respective material .50 cm from the interface, has a piece of standard heat shrink placed around it to maintain electrical isolation. The working electrode lead is then wrapped around tube A to the very top. The reference electrode is a silver wire (28 gauge) that is placed in the center of tube A. In the tube is the internal reference solution of 4M KCl with saturated silver ion. The silver wire has been coated with silver chloride to provide the necessary Ag/AgCl reference electrode.

Electrochemical Cell Materials

The pyrex glass fittings were purchased from Fisher Scientific Company, Fairlawn, N.J., 07410. The graphite rods were purchased from MCB Reagents, Cincinnati, Oh., 45212. The heat shrink for both cells was purchased from DIGI-KEY Corp., Thief River Falls, MN, 56701. The continuous vacuum triple distilled mercury came from Bethlehem Apparatus Co., Inc., Hellertown, PA, 18016. The glass tubes and NMR tubes came from Wilmad Glass Co., Buena, NY, 08310.

The glass frit filter disc with a porosity E, came from Ace Glass Inc., Vineland, N.J., 08360. The Vycor also came from Fisher as well as the internal reference solution for both reference electrodes. The silver epoxy was purchased from Acme Chemical & Insulation Company, New Haven, CT, 06505. The reticulated vitreous carbon 100 pores per linear inch, was purchased from Atomergic Chemetals Corp., Plainview, NY, 11803.

Apparatus

Cyclic Voltammetry Cell I

Cyclic voltammetry was performed using an EG & G Princeton Applied Research model 364 Polarographic Analyzer (PAR, Princeton, N.J., 08540), a Sargent-Welch XT-Y recorder (Sargent-Welch, Skokie, IL, 60077), and a Sabtronics model 2010 digital multimeter to follow the potential (Sabtronics, Tampa, FL, 33610). A Wavetek model 142 was employed to generate the waveform needed to cyclic voltammetry (Wavetek Inc., San Diego, CA, 92199).

pH and Electrode Potential Measurements

A Sargent-Welch pH meter model 6000 was used to measure the pH of the electrolyzed and non-electrolyzed solutions. It was also used to measure the potential of the reference electrode in cell II.

Resistance Measurements Cell II

A Fluke model 8060A multimeter (John Fluke MFG., Co. Inc., Everett, WA, 98206) was used to measure the potential between the

working electrode and reference electrode and also between the working electrode and the auxiliary electrode.

Controlled Potential Electrolysis/Non-spinning

A Bioanalytical Systems potentiostat model SP-2 (BAS, West Lafayette, IN, 47906) was used to supply the constant potential to the working electrode. The current vs. time plot of the controlled potential electrolysis experiment was recorded on a Sargent-Welch XT-Y recorder. A Sabtronics multimeter 2010 was used to monitor the potential.

Controlled Potential Electrolysis Spinning

A Bioanalytical Systems potentiostat model SP-2 was used to supply the potential. The output was recorded on a Sargent-Welch XT-Y recorder. The potential was monitored on a Sabtronics model 2010 multimeter. The spinner assembly was used to simulate spinning was taken from a Varian NMR probe (Varian Associates, Palo Alto, CA, 94303).

Cyclic Voltammetry Cell II

Cyclic voltammetry was performed using a Bioanalytical Systems potentiostat model SP-2 and a EG & G PARC model 175 universal programmer (PAR, Princeton, N.J., 08540) to supply the waveform. The potential was monitored with a Sabtronics multimeter model 2010 and the experimental output recorded on a Sargent-Welch XT-Y recorder.

CHAPTER IV

EXPERIMENTAL

Electrochemical Cell I

Reagents

Deionized water was used to prepare all solutions. All
chemicals were analytical reagent grade. Supporting electrolytes
were .1 M phosphate buffer and .1 M KCl. The pH of the buffer was
7.4. Stock solutions of 20 M $K_4FE(CN_6)$ were made up daily. Flami-
nox, a polarographic detergent (surfactant, furnished by Fisher
Scientific) was used.

Procedure

All experiments were conducted in solutions of .1 M KCl
and buffered with a phosphate buffer to a pH of 7.4. The $K_4Fe(CN_6)$
used as noted above was reagent grade and was used directly.
Before the addition of $K_4Fe(CN_6)$, the electrode was treated with
.1 mL of flaminox and cycled between 1.0 volts and – 1.0 volts
with the supporting electrolyte present, for approximately 10 minutes.
This was done initially to observe the potential window and after
each experiment to try to reduce the background currents to a lower
and constant value.

The buffered solution was deaerated with nitrogen for 15
minutes. All experiments were conducted at ambient temperature

(26 $\pm$ 1). Current-potential curves (cyclic voltamograms) were obtained vs. a Ag/AgCl reference electrode with a graphic working electrode during the situ oxidation and reduction of $K_4Fe(CN_6)$.

Cyclic Voltammetry

Initially 1.0 mL of buffered solution, dissolved in supporting electrolyte, was introduced into tube B or the NMR tube. Tube A was introduced into the solution so the fritted graphite W.E. was in contact with the solution. Initially, the cycling of the potential was not accompanied by spinning. In this case it was possible to observe the diffusion flow patterns of the electroactive substances.

The initial experiment involved slowly cycling the potential (1 mv/sec) to observe the colored flow patterns due to electrolysis. The corresponding patterns were next observed when the cell was spinning, and compared to the flow patterns observed by Richards and Evans.[42] These flow patterns are an important consideration when determining the efficiency of mass transport, and therefore overall electrolysis.

Forced convection, or spinning, of solid electrodes can cause variations in the current as a result of poor diffusion. This is basically the result of a non-linear concentration gradient. These non-uniform diffusion flow patterns occurred as a result of air bubbles surrounding the electrode and a non-concentric alignment of tube A. These bubbles caused large, nonreproducible variations in current during subsequent cycles.

Additional experiments were conducted with more surfactant (about .1 mL) and more careful attention was paid to the introduction of inner tube A to avoid trapping air bubbles therein. The position of tube A was also modified to get optimum alignment, and thus more uniform current distribution as a result of more symmetrical alignment. It was concluded that if Hg pool was used as a working electrode, the generation of symmetrical potential fields was possible but for this cell the position and shape of the auxiliary electrode interferred with efficient current symmetry.

Cyclic voltamograms were run on 20 mM solutions of $K_4Fe(CN_6)$ to determine the efficiency of the first cell. The cyclic voltammetry experiments were run at a scan rate of 20 mv/sec, with a rotational speed of the cell of approximately 100 Hertz. Experiments were conducted over a period of five months using the same electrode, cleaning it with dilute nitric acid prior to each experiment. The cyclic voltamograms produced revealed lack of reproducibility of current during the experiments. An attempt to resolve this was to reduce the solution and to decrease the spinning velocity. The continued variation in current indicated poor geometry, or possibly poor diffusion from the electrode. Adsorption on the electrode surface was also considered a possibility. The results did however show that voltamograms that were highly reversible in a given experiment but that, as the carbon aged, a potential lag occurred.

pH and Electrode Potential Measurements

A Sargent-Welch pH meter was used to measure the pH of the buffered phosphate solution. pH measurements were also conducted on the electrolyzed and non-electrolyzed solutions, with and without the buffer, to measure the effect of electrolysis. The pH meter was also used to measure the potential of the reference electrode vs. a saturated calomel electrode in a 1 M KCl solution similar to experimental conditions.

Initially solutions of 25 mM and 50 mM were introduced into electrochemical cell I, and cyclic voltammetry was performed. The pH measurements were conducted on the solutions before and after the experiment to see the effect on the unbuffered solutions. A non-reversible color change was noted and a substance precipitated that potentially could interfere with diffusion to and from the electrode. The current response was monitored closely to see if other environmental conditions changed as a result of the pH shift.

Electrochemical Cell II

pH and Electrode Potential Measurements

The procedure for pH measurements and the exploration of other experimental parameters are the same as those used in cell I. Proper monitoring of potential was again necessary to determine if the design parameters were acceptable. The reference electrode (Ag/AgCl) potential was checked using a second standard electrode (SCE).

It should be noted that the reference electrode was remade each week. The procedure for making and maintaining a Ag/AgCl reference electrode is given in Appendix A.

Resistance Measurements

Resistance measurements were also undertaken to evaluate cell design, to optimize the supporting medium, and to study the effect of forced convection upon the cell.

The cell was prepared for resistance measurements by allowing the electrode material to equilibrate. After equilibrium, 1.00 mL of a supporting electrolyte was added to the NMR tube. The electrode, depending on the experiment, may have been treated with a surfactant. The working electrode was introduced into the NMR tube, which in turn was lowered into the internal cavity of the auxiliary electrode. The NMR tube was positioned approximately .1 cm above the auxiliary electrode. This distance needs to be accurately repeated in each experiment. The working electrode was placed .40 cm into the solution, both of these distances being very important to reproduce to get comparable cyclic voltamogram. Both external and internal solution levels need to be reproduced as well. The resistances were measured with a Fluke multimeter, Model 8060A.

The first resistance measurement experiment utilized four concentrations of supporting electrolyte, which were checked between the working and auxiliary electrodes. The KCl supporting electrolyte was checked by determining its resistance between the

working and reference electrodes. The results revealed two basic guides that governed the pattern of the remaining resistance measurements experiments.

The results of the first resistance measurements showed that the resistance is a linear function of the concentration, which is not supporting on Ohm's Law grounds. However, a much higher electrolyte concentration was found necessary in all experiments (1 M KCl) than is usually the case. (Normally millimolar concentrations of electroactive species require .1 M concentrations of supporting electrolyte.) Secondly, the measurement of resistances between the working and auxiliary electrodes, and the working and reference electrodes, showed sufficiently consistent data that continued measurement of both experimental parameters was justified.

A second set of resistance measurements used the four concentrations of supporting electrolyte. The same electrode parameters were considered. The difference was that the NMR tube was spinning at approximately 60 Hertz.

The third and fourth experiments involved testing two different surfactants, Brij-35 and Triton-100, respectively. The experiments were conducted non-spinning. Approximately .1 mL of surfactant solution (mM) was added to each 1 mL of electrolyte solution.

The fifth experiment used Brij-35 and the NMR tube was spinning. The spin rate was approximately 60 Hertz. All other experimental parameters remained the same.

Controlled-Potential Electrolysis, Non-spinning

A controlled potential was applied to the various systems, and the current decay was monitored as a function of time. In our case an oxidizing potential was applied to various concentrations of $K_4Fe(CN_6)$. The aim of such an experiment is to characterize the behavior of the electrochemical cell in terms of electrode dimensions, cell geometry and the rate of mass transfer by the overall efficiency of the electrolysis.

To measure the efficiency of operation of an electrochemical cell, a chronoamperometry is performed in which the current will at first decrease but will reach a limiting constant value under constant voltage. If only one reaction is occurring, the current efficiency is assumed to be 100%. Then the current-time curve can be predicted since the rate of mass transfer of the electroactive species to the electrode surface limits the rate of reaction. Then the current will decay according to the Lingane equation,

$$i_t = i_o e^{-kt} \tag{17}$$

where i_t is the current at time t, i_o is the initial current and k is a function of the electrode dimensions, cell geometry, solution volume and the rate of mass transfer. The value of k contains the overall efficiency of the electrochemical cell.

For a Nernst diffusion layer model, k is given by the equation,

$$k = D_o A/SV \tag{18}$$

where D_o is the diffusion coefficient of the electroactive species, A is the electrode area, V is the solution volume, and S is the thickness of the diffusion layer. The dependence of k upon these experimental parameters is complex, but the overall k will depend on electrode shape, cell geometry, and the rate of mass transfer. These can be related back to k if the experimental parameters are known.

Once k is calculated, a comparison with other known data can indicate if the cell is operating efficiently. Since this experiment is assumed to be a diffusion controlled process, the use of equations that describe linear diffusion are used to evaluate the above-mentioned electrochemical parameters. This is appropriate, since a porous flow-through electrode approximates linear diffusion.

Initially 1 mL of a $K_4Fe(CN_6)$ solution was placed in the NMR tube. The experiment was run on three different concentrations of the solutions, with a non-spinning NMR tube. Application of a potential of +.50 volts to the working electrode vs. Ag/AgCl was maintained until the electrolysis reached a steady state condition. Surfactant was added to all the solutions to facilitate mass transport.

Calculations

In order to calculate k, it is necessary to calculate the effective surface area of the electrode. This was done by graphing $it^{1/2}$ vs. t taken from the chronoamperometric graph data. The

graph was extrapolated to zero time and the zero value was used in the equation,

$$it^{1/2} = (54.5 \times 10^3) \, nAD_o^{1/2}c^b \tag{19}$$

where n is the number of moles of electrons involved in the oxidation of one mole of ferrocyanide. The data for the diffusion coefficient was taken from Adams.[43] c^b is the concentration of the ferrocyanide in the bulk solution. This above equation is a rearrangement of equation (14), with the dimensionless factors contained in (54.5 x 10^3). In order to use equation (19) appropriately, the current is expressed in microamperes, the concentration in millimoles/liiter, t in seconds, and D_o in cm^2/sec. The multiplier (54.5 x 10^3) is equal to the Faraday, 96,500, divided by $\pi^{1/2}$. The electrode area is expressed as cm^2.

Once the electrode area is found, it is necessary to estimate a value for the diffusion layer thickness (s). Equation (13) was used in the form,

$$i_L = \frac{nFAD_oC_o}{S} \tag{20}$$

where i_L is the limiting current and S is substituted for $(\pi t)^{1/2}$. It is appropriate to substitute i_L for i for a linear concentration gradient, where i_L is proportional to concentration. This relation serves as the basis for all analytical applications. The limiting current was taken from the chronoamperometric graph at the point where the decay is limited by the diffusion rate of electroactive material to the electrode surface. Since the other parameters are

known, it is possible to calculate the diffusion layer thickness.

The k value is in turn calculable from the above data. Using equation (18) and substituting all data, an example of the electrochemical calculation follows,

$$k_{.010\ M} = \frac{.632 \times 10^{-5} cm^2/sec \times .111\ cm^2}{2.3 \times 10^{-2} cm \times 1\ cm^3} \qquad (21)$$

$$k_{.010\ M} = 3.05 \times 10^{-5} sec^{-1} \qquad (22)$$

for a .010 M concentration of potassium ferrocyanide, with D_o = .632 x 10^{-5} cm^2/sec and the effective surface area of the electrode A = .111 cm^2. The diffusion layer was calculated to be 2.3 x 10^{-2} cm.

Each experiment for a particular concentration of electrolyte had its own effective surface area of the electrode, diffusion layer thickness, and its k value. The data was correlated and compared to known data as well as data from relatively accurate empirical equations.

Controlled-Potential Electrolysis, Spinning

It is possible that the efficiency of an electrochemical cell would be improved under forced convection situations of cell spinning. Thus the aim of this experiment was to reduce the value of k by forced convection, thereby increasing the cell efficiency.

Initially 1 mL of a $K_4Fe(CN_6)$ solution was placed in the NMR tube. The experiment was run on three different solution

concentrations. The NMR tube was spun at a rate of 60 Hertz. Application of an oxidizing potential of +.50 volts to the working electrode vs. Ag/AgCl was maintained until the electrolysis reached a steady state condition. Surfactant (Brij-35) was added to all the solutions to facilitate mass transport. As before, the current decay was measured against time.

Calculations

The calculations for the effective surface area and k are the same. The calculation for the diffusion layer thickness changed. This change was a result of the hydrodynamic conditions that exist at the electrode as a result of forced convection. The diffusion layer thickness was calculated according to the equation,

$$S = 1.61 \ D_o^{1/3} \ v^{1/6} \ w^{-1/2} \qquad (23)$$

where v is the kinematic viscosity taken from Adams and $w = 2\pi N$ where N = 60 rpm.

The data was correlated with other known data as well as that generated from the nonspinning controlled-potential electrolysis experiment.

Cyclic Voltammetry

Reagents

Deionized water was used to prepare all solutions. All chemicals were analytical reagent grade. The supporting electrolyte used for all solutions was 1.0 M KCl. A 0.1 M phosphate buffer was

employed for some experiments. The stock solutions of each $K_4Fe(CN_6)$ were made up daily. A polarographic detergent, Brij-35, was used for all experiments.

<p align="center">Procedure</p>

All experiments were conducted in solutions of 1.0 M KCl with some solutions buffered with a phosphate buffer to a pH of 7.4. The ascorbic acid, ninhydrin and the potassium ferrocyanide were reagent grade as noted above and were used without assay or further purification. Before the addition of any electroactive solution, the electrode was treated with 0.1 mL of Brij-35 and cycled between 1.2 volts and - 1.2 volts with the supporting electrolyte, for approximately 10 minutes. This was done initially to observe the potential window, and thereafter to reduce the background currents and equilibrate the electrode.

The solutions were deaerated with nitrogen for 15 minutes. All experiments were conducted at ambient temperature $(26 \pm 1)^o$ C. The current-potential curves were obtained vs. a Ag/AgCl reference electrode with a RVC working electrode.

<p align="center">Cyclic Voltammetry Experiments</p>

Cyclic voltammetric experiments were employed as a method to characterize the electrochemical behavior of electrochemical Cell II. A known redox couple such as $K_4Fe(CN_6)$ can be placed into the electrochemical cell and the potential can be cycled, looking for the redox potentials for this particular couple. These

measured redox waves are then compared to literature values as before to establish proper cell function. These waves can also be used to determine if equilibration has occurred. Essentially the redox potentials of a known system are used as a standard for the cell.

Cyclic voltammetry establishes whether an electrochemical cell is operating efficiently by noting if the current-potential curves are 95-97% reproducible after 10 scans. Cyclic voltammetry can also be used to determine the potential drop by determining the peak separation of the redox potentials. Both of these measurements show the utility of cyclic voltammetry in evaluating cell design.

Most important is the ability of cyclic voltammetry to prove the existence of free radicals, and estimate their lifetimes.

Initially 1 mL of a .050 M solution of $K_4Fe(CN_6)$ that had been dissolved in 1.0 M KCl was placed into the NMR tube along with .1 mL of Brij-35. The working electrode was introduced into the NMR tube concentrically, with .4 cm of the RVC in the solution. Cyclic voltammetry was performed on this solution to determine the redox potentials and to compare them to the literature.

Eventually cyclic voltammetry was performed on solutions of $K_4Fe(CN_6)$ with various concentrations (.010 M, .025 M, and .100 M) and the redox potentials compared to the potentials obtained in the first experiment.

Experiments were conducted on other systems such as ascorbic acid and ninhydrin for verification. Both of these systems showed redox potential values quite different from each other and potassium ferrocyanide.

Experiments were conducted on .050 M $K_4Fe(CN_6)$ each morning to determine that complete equilibration of the electrode had occurred, and that the cell was operating properly.

Potential-step cyclic voltammetry experiments were performed on p-phenylenediamine using the procedure suggested by Papouchado, Bacon and Adams.[44] This was done to explore the possibility of determining the existence and stability of a free radical system.

Cyclic voltammetry was used as a way to determine if electrode aging had occurred over a three month period by comparing the cyclic voltamograms run on the standard .050 M $K_4Fe(CN_6)$ initially, and at the end of experimentation.

Mercury Coated RVC Electrode

Experiments were conducted according to the procedure of Peterson and Wong to coat mercury on the RVC working electrode.[45] This was done for two reasons. One, because mercury coated on a glassy carbon electrode has been found to expand the potential window and secondly because it may cover organic functional groups that attach themselves to glassy carbon. This shielding effect may eliminate interference of the organic functional groups that inhibit the redox reactions of aromatic organic compounds, and promote better detection of free radicals by cyclic voltammetry.

CHAPTER V

EXPERIMENTAL RESULTS AND DISCUSSION

Electrochemical Cell I

The results for the cyclic voltammetry experiments that were performed on electrochemical Cell I are represented in Figure 11 and Figure 12. Before these current-potential curves are considered, it is important that commonly used electrochemical convention be represented. Figure 10 is a guide to the convention used for plotting electrochemical data.

Cathodic current

REDUCTION

As the potential is increased in a negative direction, the electrode becomes a stronger reducing agent.

The current plotted above the line indicates a negative charge flow <u>from</u> the electrode.

E (+) volts

E (−) volts

The current plotted below the line indicates a negative charge flow <u>to</u> the electrode.

As the potential is increased in a positive direction, the electrode becomes a stronger oxidizing agent.
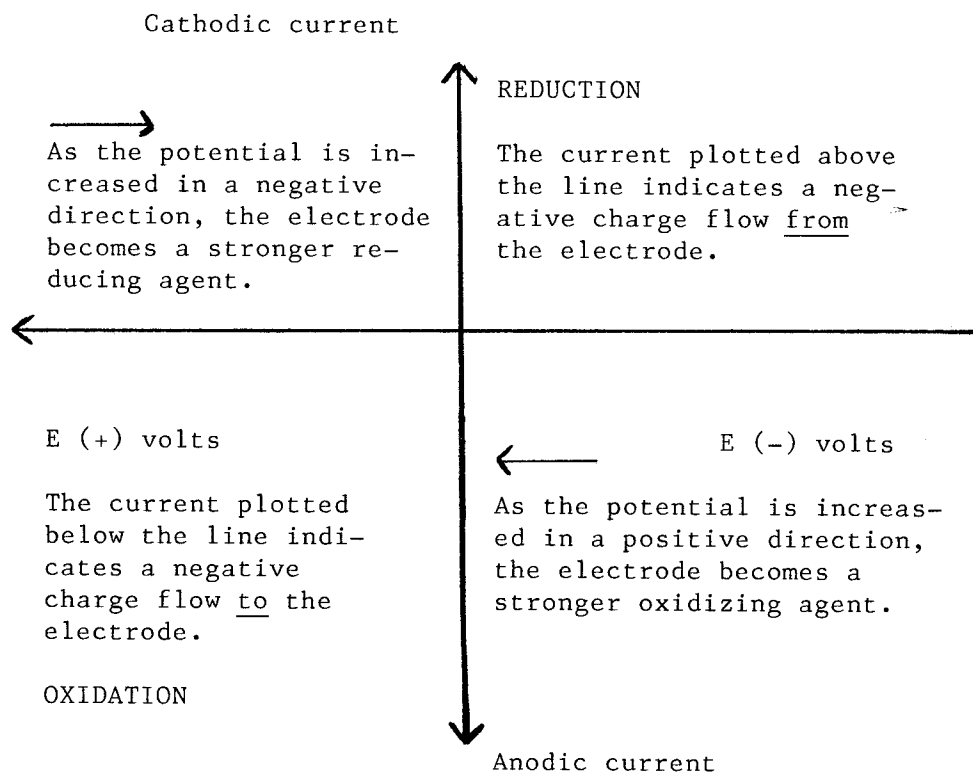
OXIDATION

Anodic current

Figure 10. Convention for plotting cyclic voltamograms.

Figure 11 indicates the cyclic voltamogram for 20 mM
$K_4Fe(CN_6)$ in 0.1 M KCl. This is the first stable "cyclic" to be
produced. It shows a lack of current reproducibility, which indi-
cates variable diffusion to the electrode. This behavior also
points to a lack of retention of the electroactive substance at
the electrode surface, which means incomplete oxidation or reduc-
tion of the electroactive species. The current reproducibility was
only 68% after only 6 scans, which is not acceptable.

The causes are considered threefold. The first cause is
considered to be poor geometry of the auxiliary electrode. The
second was forced convection to solid electrodes. In order for
steady state conditions to occur it is necessary to have rotational
rates of at least 10 Hertz to develop a steady state, diffusion
controlled process. The third cause is considered to be non-uni-
form potential fields that occur as a result of the persistent
vortex which developed during spinning. Bubbles that were present
on the sides of the electrode also contributed to the non-uniform
potential fields. Finally there was no isolation of the auxiliary
electrode from the working electrode.

The next cyclic voltamogram indicates much greater current
reproducibility. The reproducibility is of the order of 92.4%
after 10 scans, which shows that the changes made in the electrode
design were effective. Figure 12 indicates cyclic voltamograms
that are reproducible and thus reversible, which indicates that
the electrode is operating efficiently. This was a result of the

addition of surfactant and careful placement of tube A to eliminate trapping air bubbles at the side of the electrode.

pH and Electrode Potential Measurements

The results of the pH measurements for electrolyzed and non-electrolyzed solutions of $K_4Fe(CN_6)$ as well as buffered solutions before and after electrolysis are given in Table 1.

TABLE 1

pH OF ELECTROLYZED AND NON ELECTROLYZED $K_4Fe(CN_6)$

OF BOTH BUFFERED AND NON BUFFERED SOLUTIONS

Experimental parameter	pH (.025 M)	pH (.050 M)
Non-electrolyzed, initial	6.6	6.6
Electrolyzed, final	6.2	6.1
Buffered, initial	7.4	7.4
Buffered, electrolyzed	7.4	7.3

The above table indicates the necessity of a buffered solution when a controlled-potential electrolysis of cyclic voltammetry are performed. The pH shift usually becomes evident after the 5th cycle or scan.

Cell I was the culmination of much work and design consideration to prepare a cell which could be used to efficiently produce reaction intermediates in situ. Further work on cell I was abandoned because of a number of reasons. The primary reason was the lack of
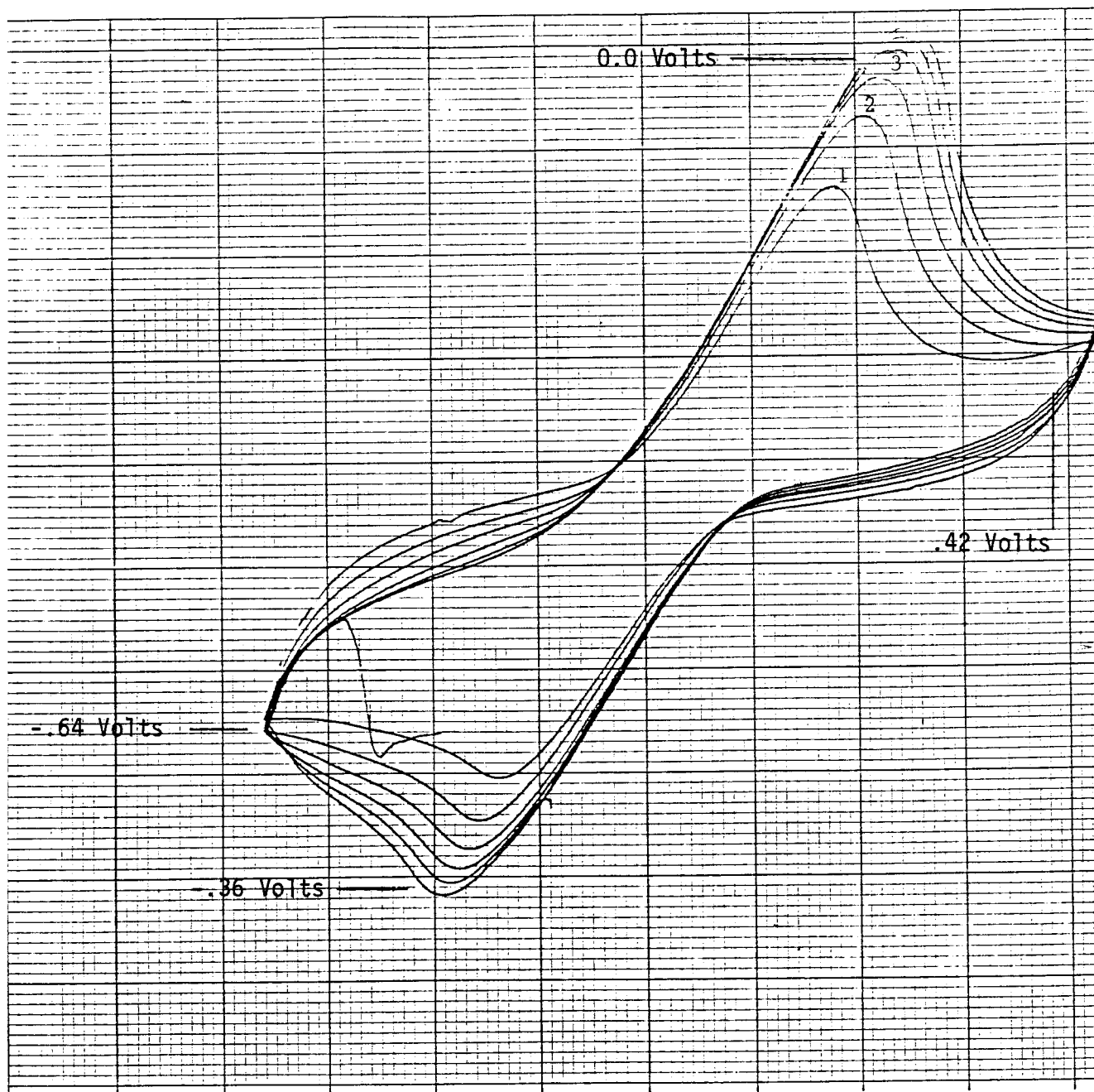
Figure 11: Cyclic Voltammograms of potassium ferrocyanide 20mM in .1M
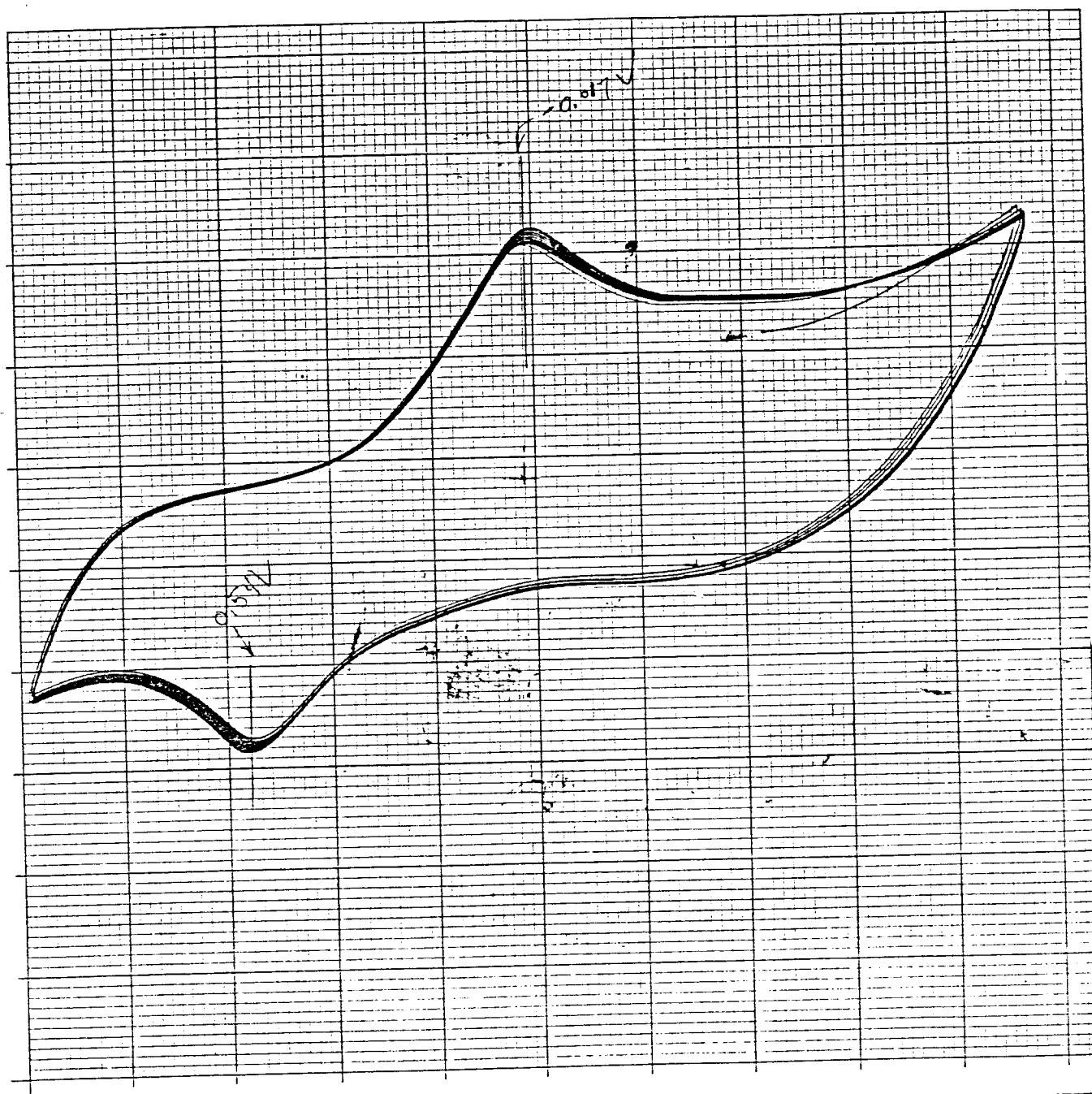KCL at a scan rate of 20mv/sec.

reproducibility of current. Also considered, was the fact that the auxiliary electrode was isolated from the reference electrode. There was a relatively large separation of 4 cm between the auxiliary and reference electrodes. Normal separations are between 0.1 and 0.2 cm. There was also a problem of the vortex, and the lack of consistent concentric operation inhibited cell operation. Potential lag eventually developed, as can be seen in the different redox potentials, between the cyclic voltagrams presented in Figure 11 and Figure 12.

Figure 12: Cyclic Voltammogram of 20mM potassium ferrocyanide in .1M
          KCl at a scan rate of 20mv/sec.

Electrochemical Cell II

pH and Electrode Potential Measurements

The results of the pH measurements in Cell II do not differ significantly from those for Cell I, shown in Table 1. The measurement of the potential of the reference electrode vs. a saturated calomel electrode experimentally was .050 volts. This compares quite well to the theorical value of .044 volts. The measurement was conducted at 25 degrees Celsius.

Resistance Measurements

The results of the resistance measurements between the working and auxiliary electrodes, and the working and reference electrodes for different concentrations of supporting electrolyte are given in Tables 2 through 6.

TABLE 2

RESISTANCE MEASUREMENTS NON SPINNING

| KCl Concentration | Resistance kohms | |
	Working-reference	Working-auxiliary
0.1 M	85.02	64.25
0.5 M	74.34	51.34
1.0 M	8.90	44.37
1.5 M	6.05	37.21

TABLE 3

RESISTANCE MEASUREMENTS SPINNING

| KCl Concentration | Resistance kohms | |
	Working-reference	Working-auxiliary
0.1 M	59.98	49.84
0.5 M	30.13	35.67
1.0 M	20.23	20.85
1.5 M	22.85	16.06

TABLE 4

RESISTANCE MEASUREMENTS BRIJ-35 NON SPINNING

KCl Concentration	Working-reference	Working-auxiliary
0.1 M	44.07	46.35
0.5 M	26.03	33.40
1.0 M	3.25	15.90
1.5 M	2.32	4.42

TABLE 5

RESISTANCE MEASUREMENTS TRITON-100 NON SPINNING

	Resistance kohms	
KCl Concentration	Working-reference	Working-auxiliary
0.1 M	30.98	32.03
0.5 M	20.74	22.87
1.0 M	19.02	26.45
1.5 M	14.15	22.32

TABLE 6

RESISTANCE MEASUREMENTS BRIJ-35 SPINNING

	Resistance kohms	
KCl Concentration	Working-reference	Working-auxiliary
0.1 M	31.35	29.96
0.5 M	18.21	8.90
1.0 M	2.95	2.87
1.5 M	2.19	2.50

For each resistance measurement experiment conducted, it was necessary to perform the equilibration procedure or the data produced would be badly skewed. The data is graphed in Figure 13 to show the resistance difference between spinning and non spinning with no surfactant present. This graph is interesting since it showed a rapid drop of resistance for the spinning measurements, but at the higher concentrations, the resistance measurements leveled off, while the non spinning resistance measurements continued to fall. Apparently in forced convection situations, a leveling off as an inherent resistance develops, unrelated to diffusion.

Figure 14 is a typical representation of the non spinning cell, which shows also the effect of adding surfactant and spinning.

Figure 15 is a comparison of the two surfactants.

A resistance value of 2.95 kohms for the spinning cell with the surfactant (Brij-35) is acceptable. The literature value for porous flow-through electrode with a spinning cell is 2 kohms.[46] (This literature cell also used reticulated vitreous carbon.) The resistance measurements showed two things. First, that surfactant can considerably lower the resistance of the electrochemical cell. Second, spinning is important to the mass transport of electroactive substances to the electrode surface.

Controlled Potential Electrolysis Non spinning

The results of data for the effective surface area of the electrode are given in Table 7.
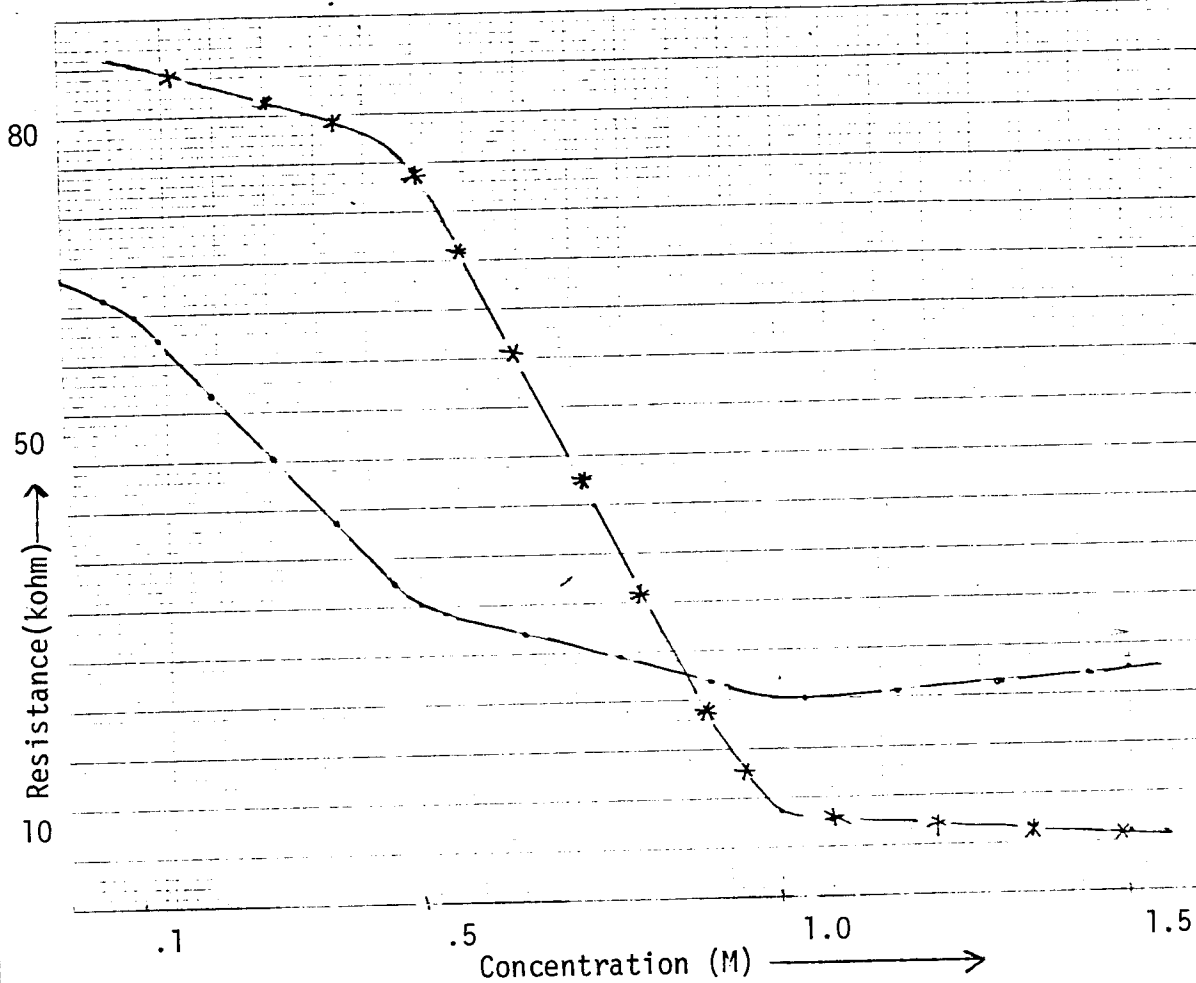
Figure 13: Resistance measurements comparing the spinning cell and the non-spinning cell. The symbol *———*———* indicates the non-spinning cell. The symbol .———·——— indicates the spinning cell.
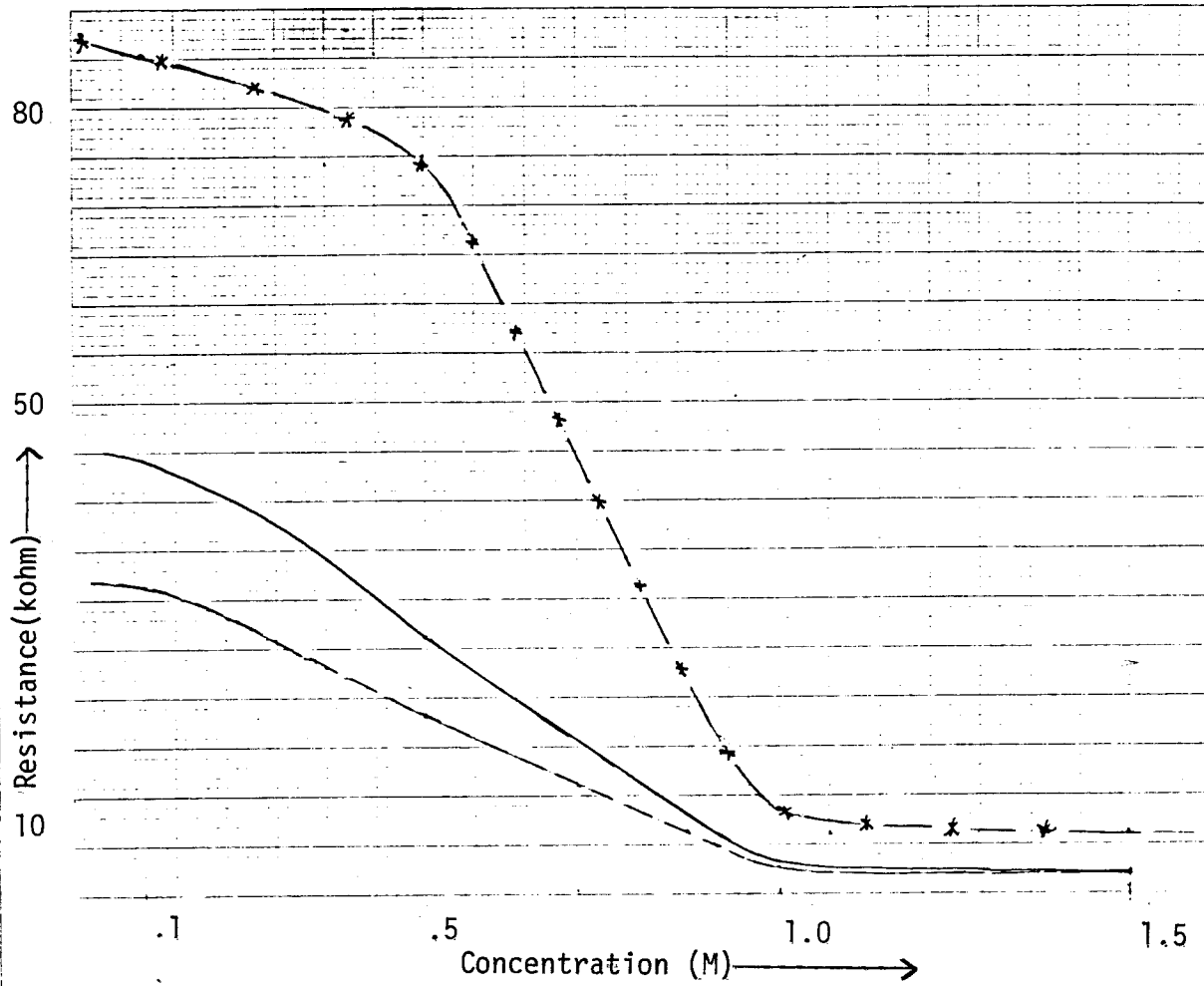
Figure 14: Resistance representing the effect of the surfactant and the surfactant and spinning on the cell with respect to the non-spinning cell. The symbol *————*————* indicates the non-spinning cell. The symbol ———— indicates the non-spinning cell with surfactant. The symbol ———————— indicates the spinning cell with the surfactant Brij-35.

Figure 15: Resistance measurements comparing the surfactants while the cell is not spinning. Brij-35 indicated by *——*——— , Triton-100 is indicated by ——— ——— .

TABLE 7

EFFECTIVE ELECTRODE SURFACE AREA

$K_4Fe(CN_6)$ Concentration	effective surface area (cm^2)
0.010 M	0.111
0.025 M	0.108
0.050 M	0.107
AVERAGE	0.108 $\pm$ 0.001

TABLE 8

DIFFUSION LAYER THICKNESS

$K_4Fe(CN_6)$	diffusion layer thickness (cm)
0.010 M	1.88×10^{-2}
0.025 M	2.28×10^{-2}
0.050 M	1.76×10^{-2}
AVERAGE	$1.97 \times 10^{-2} \pm 0.20 \times 10^{-2}$

TABLE 9

k VALUES

$K_4Fe(CN_6)$ Concentration	k values (sec^{-1})
0.010 M	3.05×10^{-5}
0.025 M	3.63×10^{-5}
0.050 M	3.84×10^{-5}

The data in Table 7 were calculated for three different con-
centrations of potassium ferrocyanide using three different i scales.
The effective surface area calculation shows reasonable consistency
in the data, indicating that the electrochemical cell is operating
consistently and efficiently. The corresponding average surface
area is 0.108 cm^2. The solution to be electrolyzes is 1 mL, so
that there is a reasonable solution volume to effective surface
area ratio. This is important because as solution volume decreases
the electrolysis rate constant k decreases, and the electrolysis
times will decrease, thereby providing more efficient electrolysis.

The diffusion layer calculation indicated an averaged value
of 1.97×10^{-2} cm for the non-spinning cell. This agrees extremely
well with comparable data of Sawyer and Roberts[47] and Adams.[48] The
diffusion layer calculation can also be compared to an empirically
derived equation that is considered to be a good approximation of
the diffusion layer thickness. The equation is,

$$S = (D_o t)^{1/2} \tag{24}$$

where D_o is the diffusion coefficient and t is the time where diffusion begins to take over after the initial decay of current. For the three experiments this value was taken to be 60 seconds. The diffusion layer thickness calculated for potassium ferrocyanide using equation (24) was 1.94×10^{-2} cm. This value is in good agreement with the electrochemically calculated value (1.97×10^{-2} cm).

One reason for considering the k values for the stationary system was to relate it to that of the spinning cell. The benefit of spinning the cell (conditions of forced convection) is revealed by comparing the k values of both experiments.

The calculations of the effective surface area of the electrode for the spinning experiment reveals excellent consistency of the data. Again three different concentrations of potassium ferrocyanide was used. The averaged value for the effective surface area of 0.096 cm^2. This value is about 0.012 cm^2 smaller than the first value for the non-spinning area. This occurred because the supporting structure of the electrode, although strong, will chip and flake causing a reduction of the surface area. This occurs mainly as a result of handling and mechanical stirring of the system. Overall, the correlation of the effective surface area data reveals excellent operating reproducibility and efficiency of the electrochemical cell.

The diffusion layer for the spinning system was calculated according to an equation which considers the hydrodynamic conditions

of the system. The correlation was a result of the forced convection and equation (23). The values are empirical ones and the correlation is a bit better.

Controlled-Potential Electrolysis, Spinning

The results of the calculations for the controlled potential electrolysis experiment spinning are given in Tables 10 through 12.

TABLE 10

EFFECTIVE ELECTRODE SURFACE AREA

$K_4Fe(CN_6)$ Concentration	effective surface area (cm^2)
0.025 M	0.096
0.050 M	0.098
0.100 M	0.096
AVERAGE	0.096 $\pm$ 0.001

TABLE 11

DIFFUSION LAYER THICKNESS

$K_4Fe(CN_6)$ Concentration	diffusion layer thickness (cm)
0.025 M	6.96 x 10^{-4}
0.050 M	6.96 x 10^{-4}
0.100 M	6.96 x 10^{-4}

TABLE 12

k VALUES SPINNING

$K_4Fe(CN_6)$ Concentration	k values (sec^{-1})
0.025 M	0.87×10^{-3}
0.050 M	0.87×10^{-3}
0.100 M	$0.88 \times 10{-3}$

The calculated values from Table 10 and Table 11 were intro-
duced into equation (18) and the result is given above in Table 12.
The k values for Cell II, spinning, are quite comparable to other
systems. The k value for a normal spinning cell, developed by
Karp and Meites, was 1.0×10^{-3} at s^{-1} 600 rpm.[49] This is
approximately 0.0013 seconds different than the present Cell II
spinning at 60 rpm, or only 10% as fast as the spinning rate as
the Karp and Meites cell. Bard was able to produce k values of
1.2×10^{-2} s^{-1} for a cell spinning at 1800 rpm or a relatively
normal speed for an NMR tube.[50] k values that increase under forced
convection conditions, or spinning, decrease the electrolysis time
and thereby increase the operating efficiency of the electrochemical
cell.

This investigation has shown that it is possible to improve
the k values an order of magnitude with the cell operating at low
speeds by suitable change in cell geometry and operating conditions.

The k values are roughly the same as those for a cell operating ten times as fast. The spinning experiment also shows high operating efficiency, thereby demonstrating the beneficial effect of spinning on cell efficiency.

The results of the cyclic voltammetry experiments performed with Cell II are shown by Figure 16 through 27. Note that Brij-35 is used as surfactant in all these cases.

Figure 16 through Figure 19 show a high cell resistance during the initial experiments, characteristic of electrodes. In order to decide which electrode(s) were the cause, the cell was run using a different reference, auxiliary, and working electrode. It was found that the electrode of high resistance was the working electrode, composed of RVC and copper wire. Since the RVC auxiliary electrode functioned very well in previous independent experiments, RVC was probably not the cause. The ohmic contact between RVC and copper is suspect.

Figure 17 and Figure 18 show more characteristic redox potentials and peak formation. This was accomplished by eliminating solution contact with the copper wire. The H_2O-copper interface apparently created a high resistance. Current is maintained efficiently with the copper-RVC contacted by silver epoxy.

Figure 19 shows that the initial cyclic voltammogram was reproducible, and shows the literature redox potentials. This occurred after addition of silver epoxy was placed around the copper wire and on the RVC. Figure 20 displays an experiment using
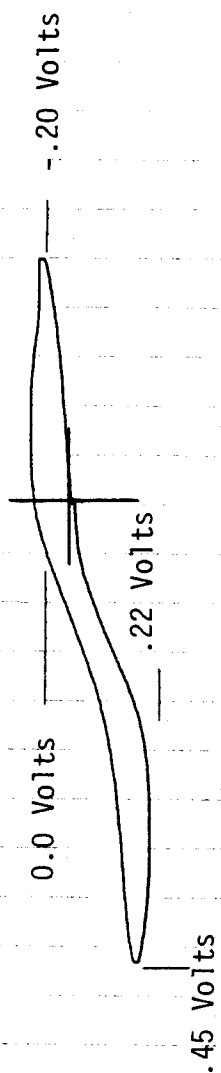
Figure 16: Cyclic Voltammogram of 50 mM potassium ferrocyanide in 1.0 M KCl. The scan rate was 50 mv/sec with a current range of 50 mA. This is a classic representation of high cell resistance.
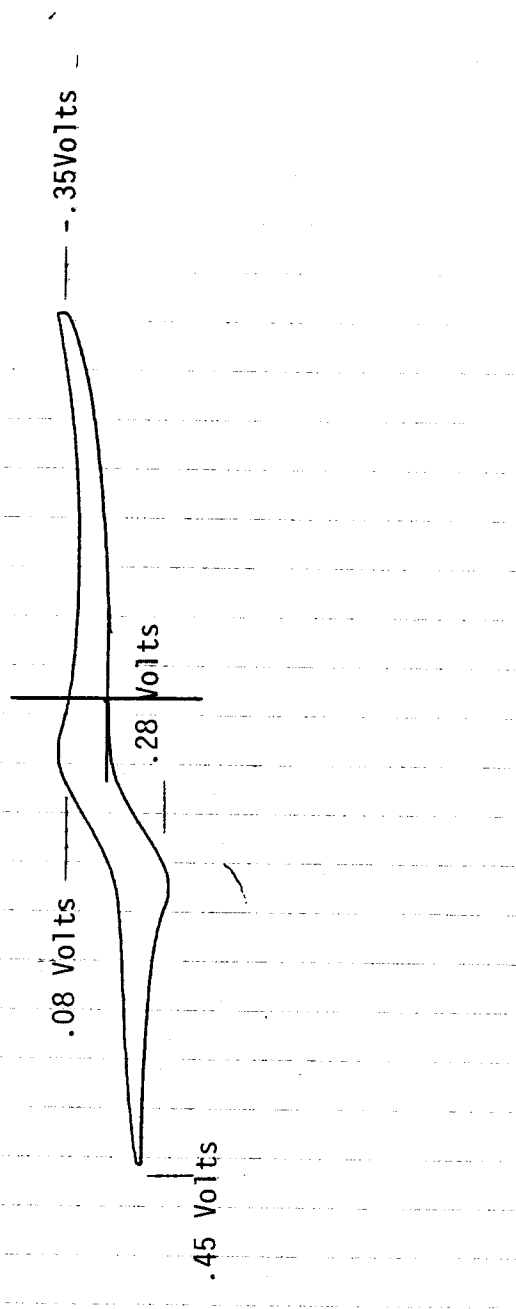
78

Figure 17: Cyclic Voltammogram of 50 mM potassium ferrocyanide
in 1.0 M KCl. The scan rate was 20 mV/sec with a
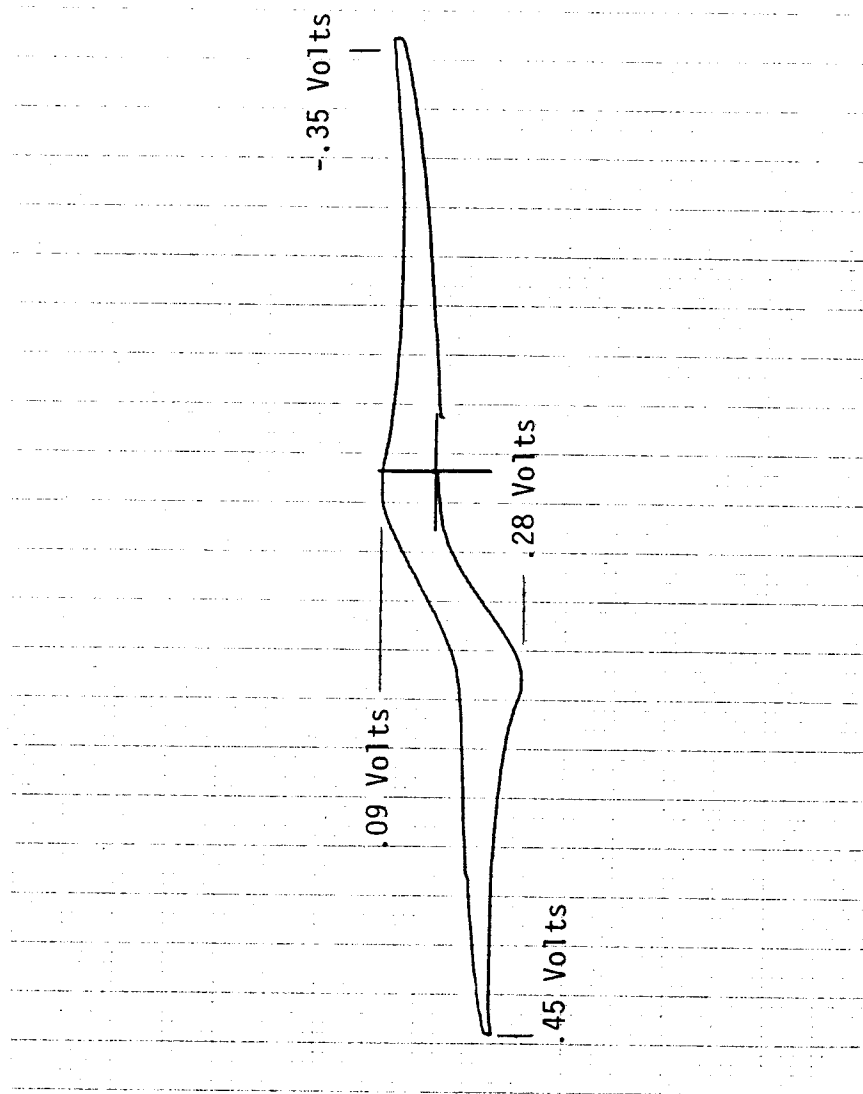current range of 50 mA. Note redox potentials with
respect to Figure 16.

Figure 18: Cyclic Voltammogram of 50 mM potassium ferrocyanide in 1.0 M KCl. The scan rate was 50 mV/sec with a current range of 50 mA.
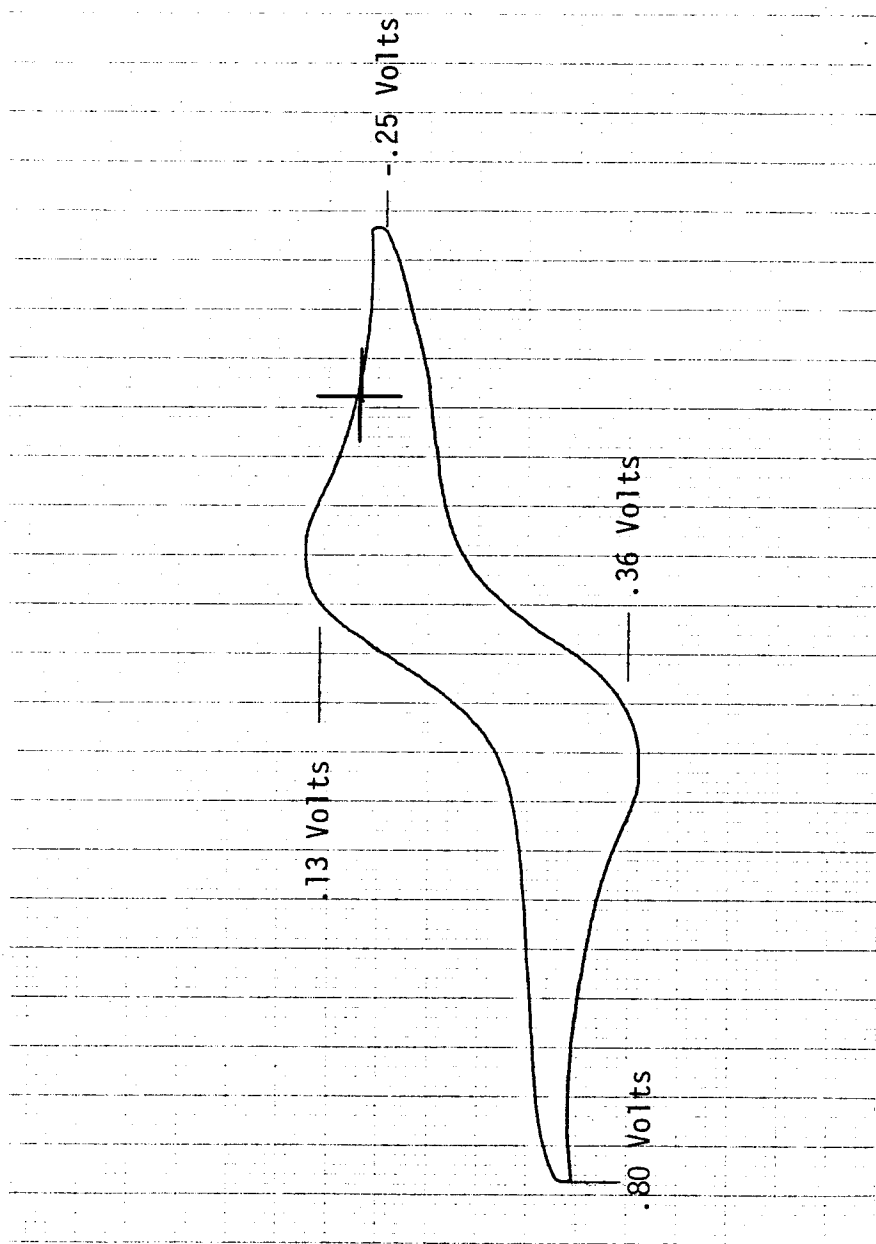
80

Figure 19: Cyclic Voltammogram of 25 mM potassium ferrocyanide
in 1.0 M KCl. The scan rate was 20 mV/sec with a
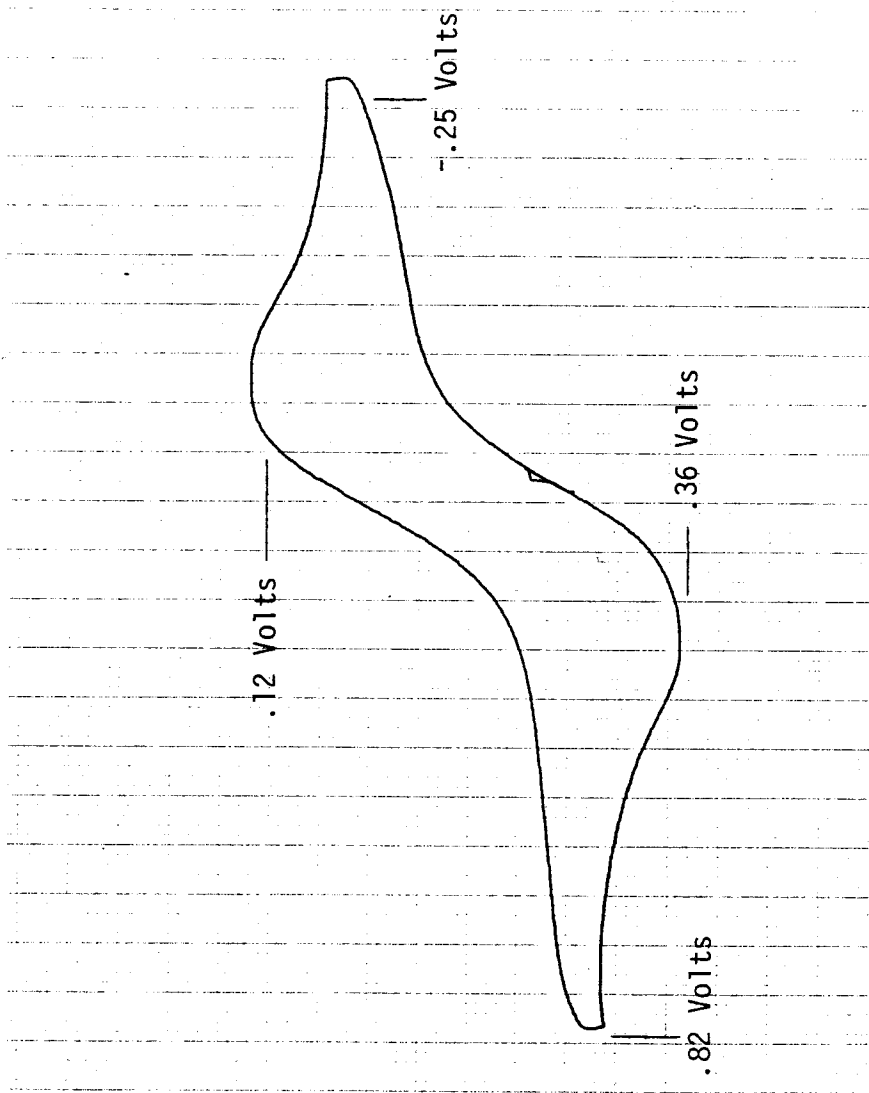current range of 20 mA. Note redox potentials.

Figure 20: Cyclic Voltammogram of 25 mM potassium ferrocyanide
in 1.0 M KCl. The scan rate was 50 mV/sec with a
current range of 20 mA.

a faster scan rate to see if the redox potentials would be repro-
duced, or a potential lag would occur. Figure 20 and Figure 21
indicate that the scan rate had no effect on the redox potentials
or potential lag.

Figure 21 is an example of the standard cyclic voltammo-
gram used to characterize the operating behavior of the electro-
chemical cell. The redox potentials were compared to literature
values to determine if the cell was operating properly. Norvell
and Mamantox reported values of 0.328 Volts for the oxidation of
the ferrocyanide and 0.130 Volts for the reduction of ferricyanide
vs. SCE.[51] Sleszynski and Osteryoung reported values of 0.336 Volts
for the oxidation of ferrocyanide and 0.130 Volts for the reduction
of ferricyanide vs. an SCE. The values obtained by this study are
vs. a Ag/AgCl reference electrode. With a theoretical difference
of 0.044 Volts between SCE and Ag/AgCl, the above-reported litera-
ture values of 0.328 Volts and 0.336 Volts for the oxidation of
ferrocyanide become 0.372 Volts and 0.380 Volts vs. a Ag/AgCl.
Note Appendix C for Electrode Convention.

The above values indicate excellent agreement with the
oxidation potential of 0.37 Volts found in Figure 21. A value of
$\pm$ 0.020 Volts vs. literature is considered good.[53] All redox
potentials were reported using RVC as the electrode material with
potassium ferrocyanide in KCl as the chemical system investigated.

Figure 22 and Figure 23 are cyclic voltammetry experiments
that were conducted using slow scan rates. This was done to
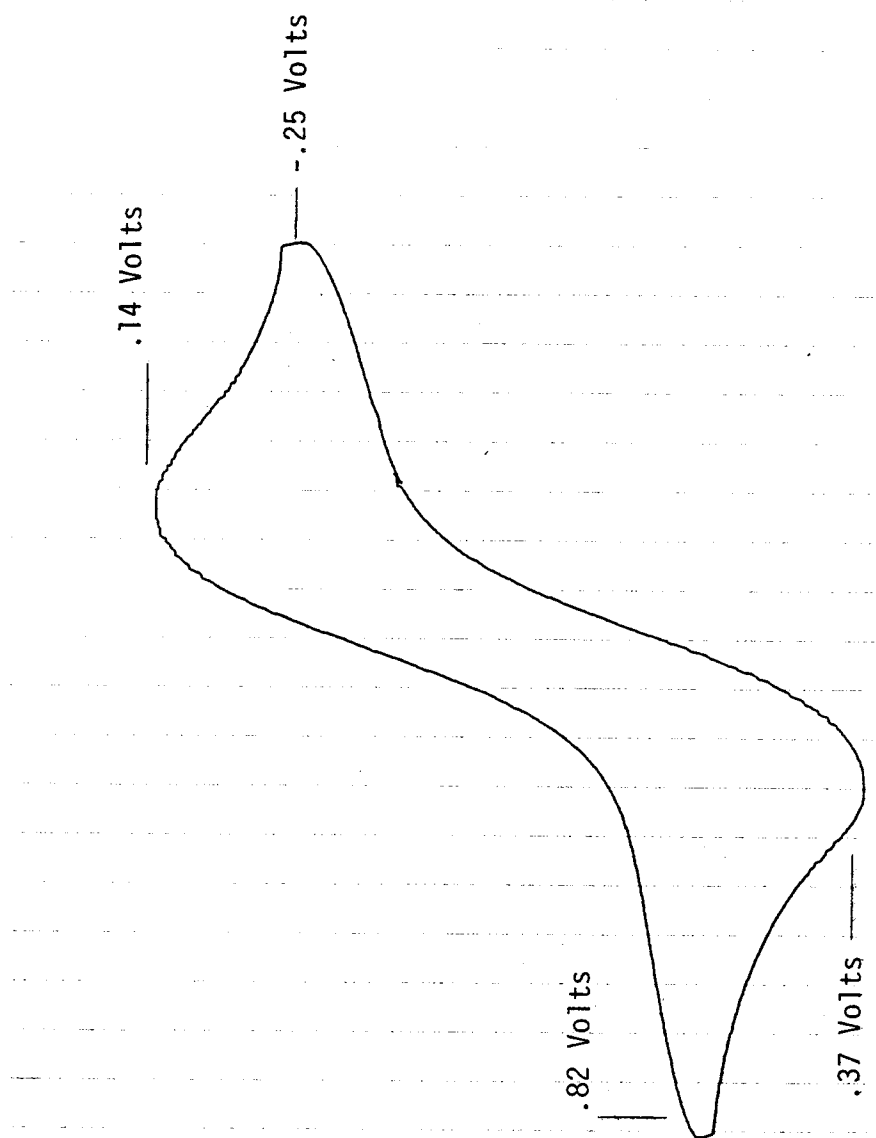
83

Figure 21: Cyclic Voltammogram of 25 mM potassium ferrocyanide
in 1.0 M KCl. The scan rate was 50 mV/sec with a
current range of 20 mA. This cyclic voltammogram
is the standard to characterize the operating be-
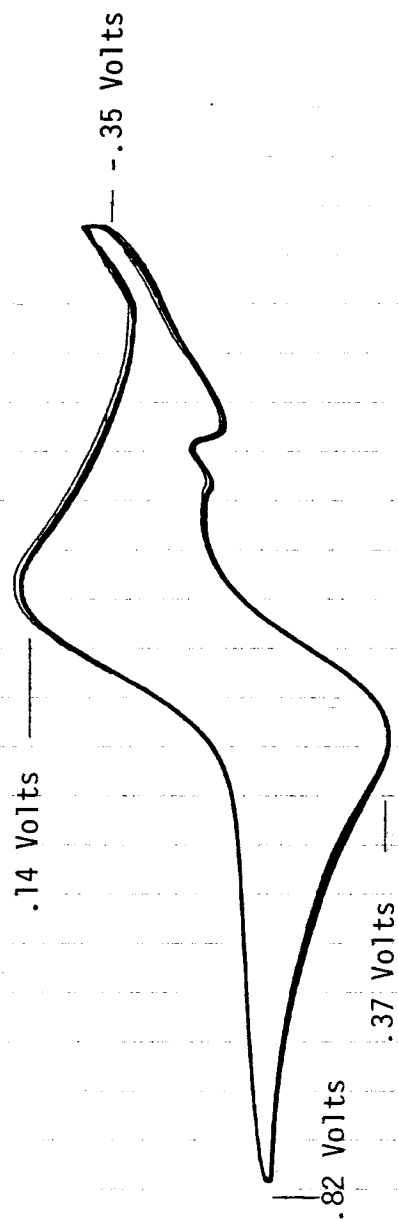havior of the electrochemical cell daily.

Figure 22: Cyclic voltammogram of 25 mM potassium ferrocyanide
in 1.0 M KCl. The scan rate was 5 mV/sec with a
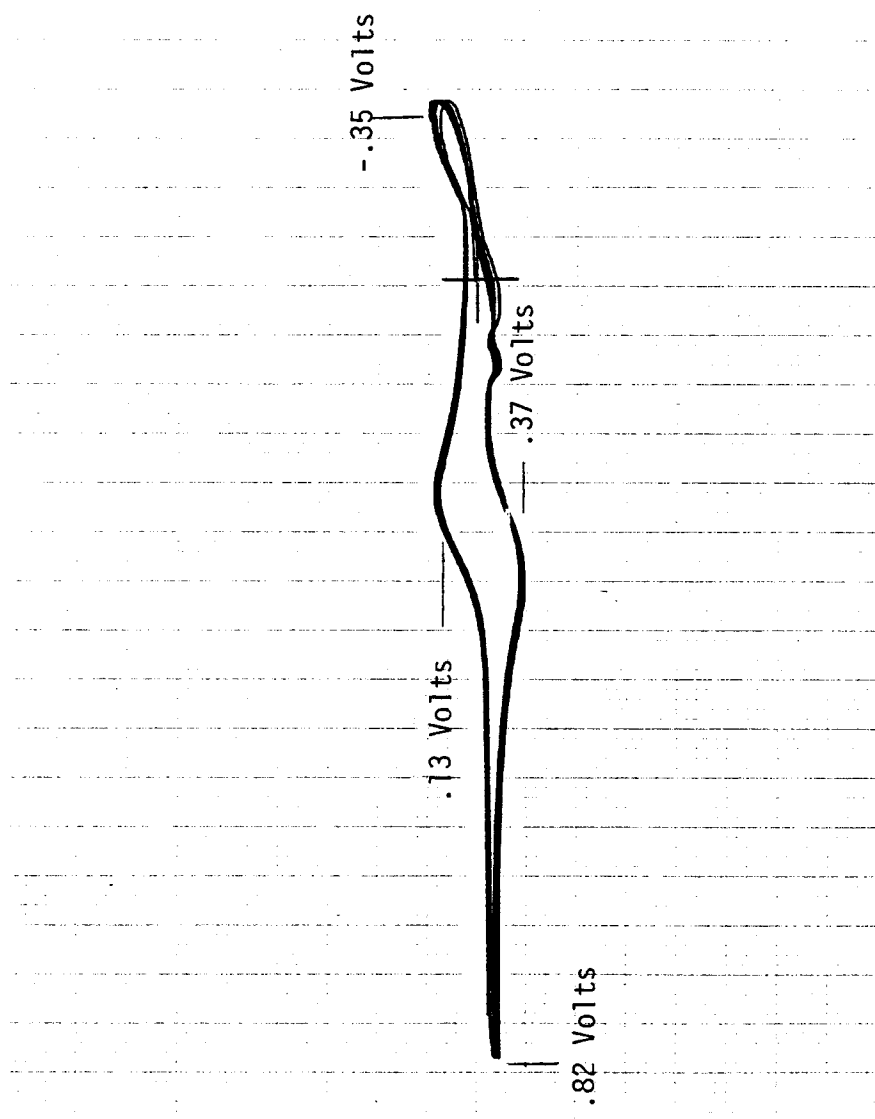current range of 20 mA. Source of glitch unknown.

Figure 23: Cyclic Voltammogram of 25 mM potassium ferrocyanide
in 1.0 M KCl. The scan rate was 2 mV/sec with a
current range of 20 mA.

indicate a possible shift in the redox potentials. There was no shift. Experiments were also run on different concentrations of potassium ferrocyanide (0.010 M, 0.050 M, and 0.100 M) to detect any possible potential shifts. The redox potentials of each of these systems were consistent with the redox potentials of Figure 21.

Figure 24 and Figure 25 are cyclic voltammetry experiments that were run on electroactive biological compounds. These experiments were conducted for two reasons. One, to provide evidence that the oxidation and the reduction peaks observed are not a result of oxygen or hydrogen dissolved in the solvent. Secondly, to view the behavior of aromatic biological compounds using RVC. Note the possible adsorption of ninhydrin on the electrode in Figure 25. This may be a result of organic functional groups that attach themselves to the surface of the RVC.

Figure 26 is the cell standard. This diagram is most important for two basic reasons. Primarily, that the cell was reproducibly operating after a period of three months. Secondarily, that the equilibration procedure was successful in providing longterm use of RVC. As far as is known we are the first group to regenerate RVC and use it longer than a week without potential lag or electrode breakdown. Electrode breakdown is usually noted by complete instability of the cyclic voltammetry plot.

Figure 27 is an attempt to resolve by cyclic voltammetry the cation radical of p-phenylenediamine to indicate its existence and attempt to quantify stability. The experiment was performed at
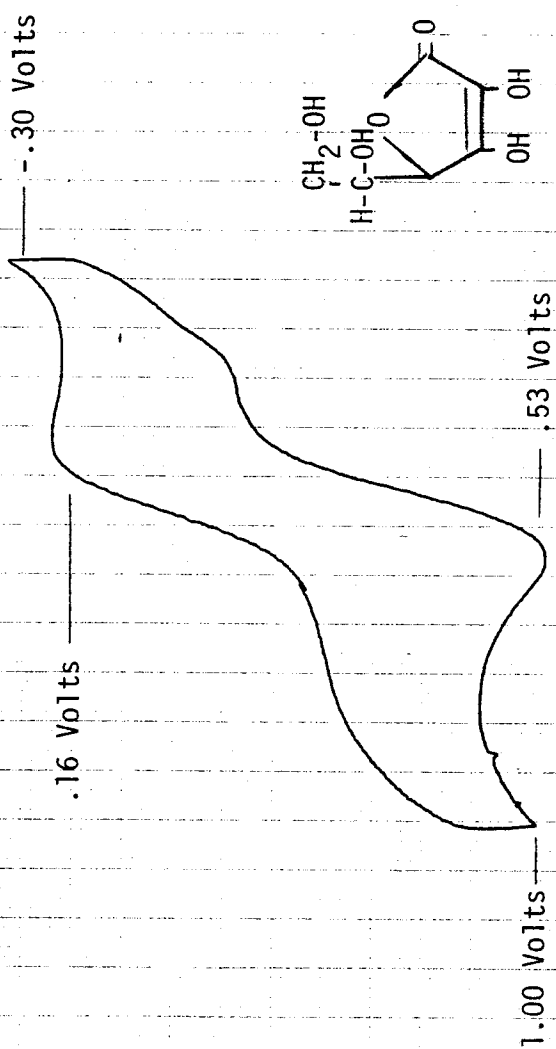
Figure 24: Cyclic Voltammogram of 20 mM ascorbic acid in 1.0 M
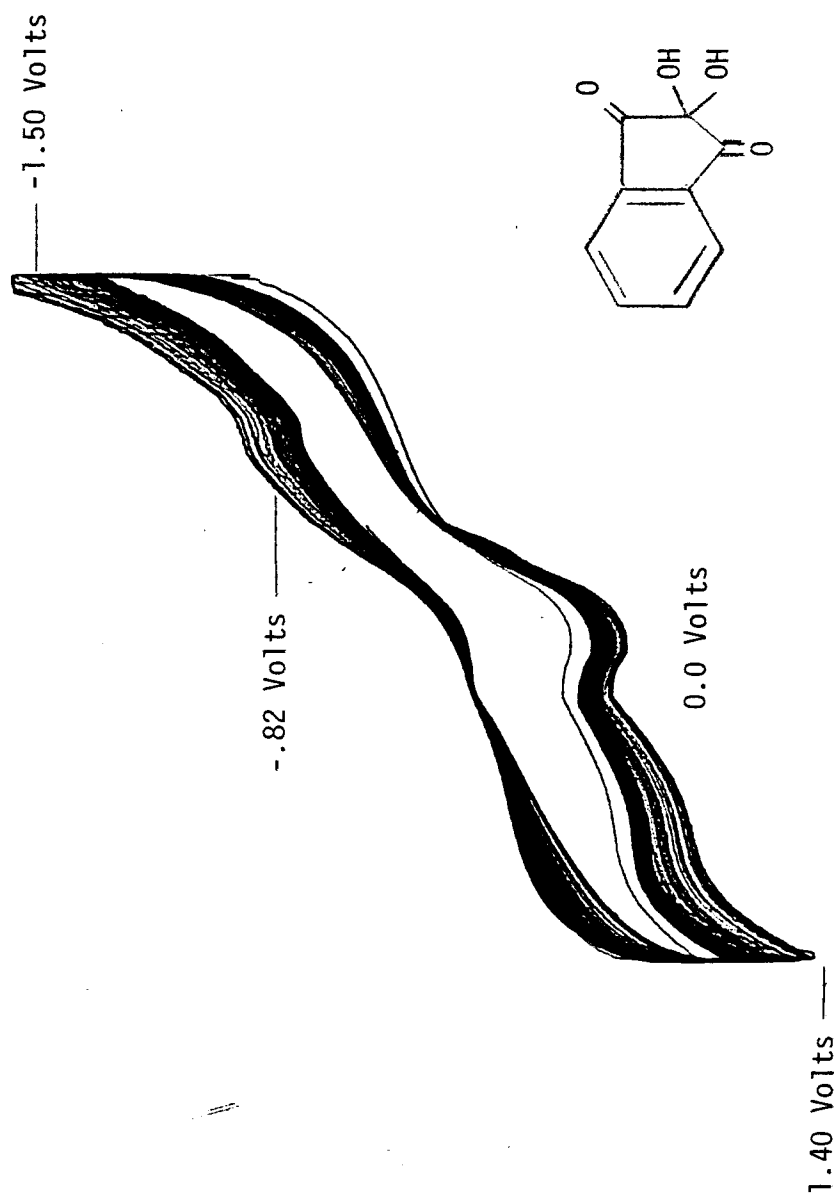KCl. The scan rate was 50 mV/sec with a current
range of 10 mA.

Figure 25: Cyclic Voltammogram of 20 mM ninhydrin in 1.0 M KCl. The scan rate was 20 mV/sec with a current range of 20 mA. Note that the diagram indicates possible adsorption on the electrode.
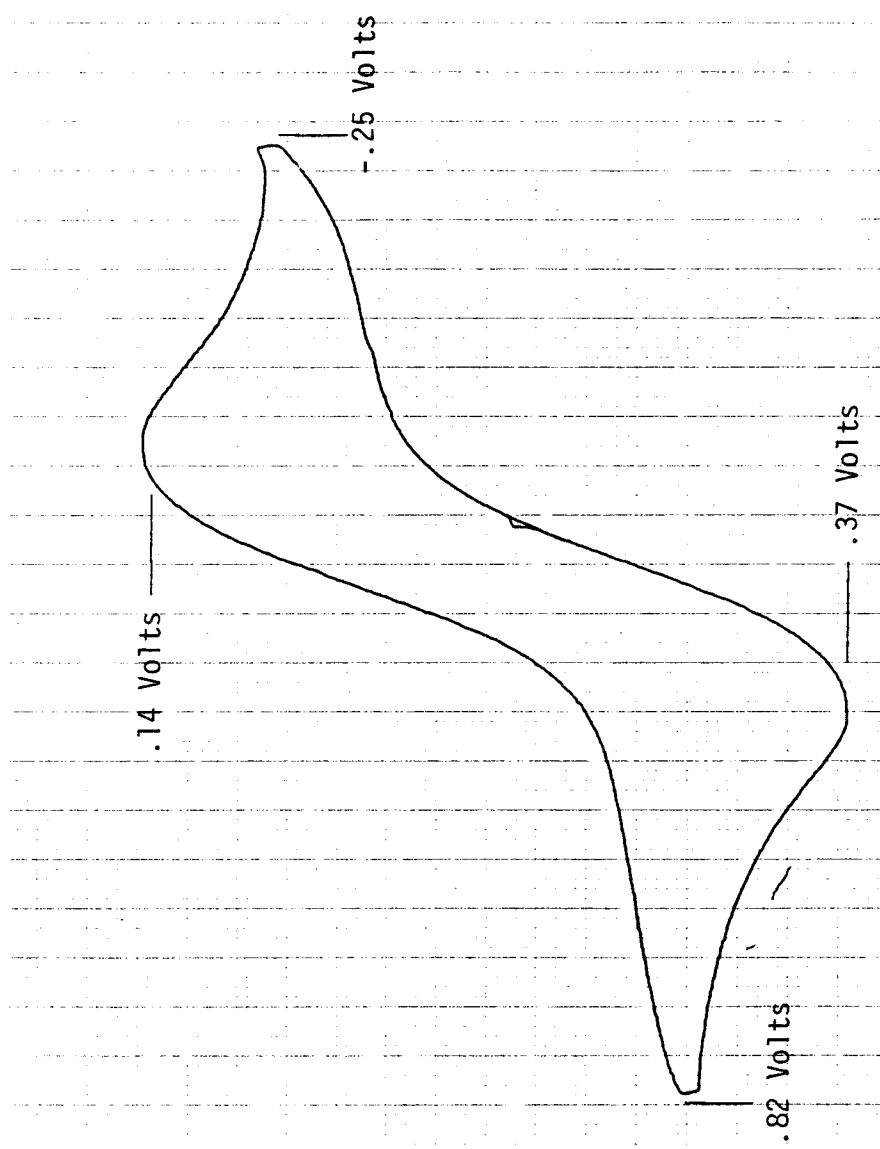
Figure 26: Cyclic Voltammogram of 25 mM potassium ferrocyanide in 1.0 M KCl. The scan rate was 50 mV/sec with a current range of 20 mA. This diagram indicates the reproducibility of consistent electrochemical cell operation as well as evidence for longterm possible use of reticulated vitreous carbon.
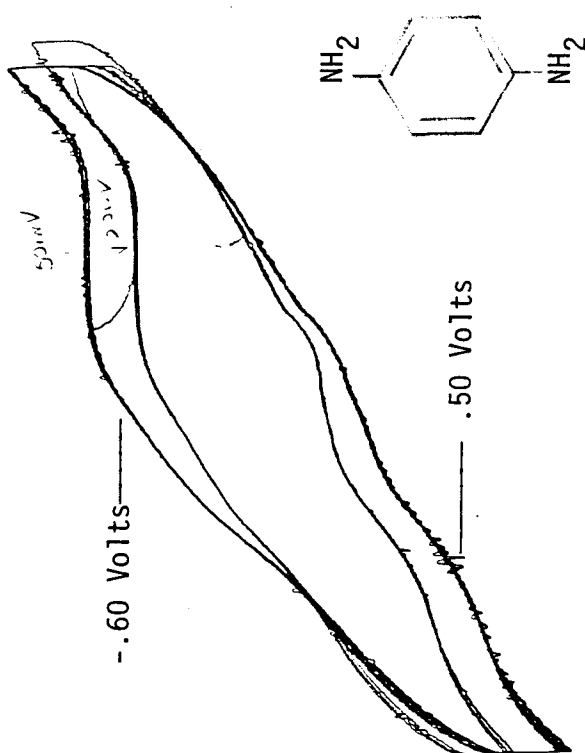
Figure 27: Cyclic voltammograms of 25 mM p-phenylenediamine in
1.0 M KCl. As indicated the scan rates were 20 mV/
sec and 50 mV/sec with a current range of 20 mA.

two different scan rates to determine if the transient species reacted too fast to be seen. Although possible evidence is suspected by the slight potential at 0.50 Volts no conclusion can be made.

Figure 28 displays the use of potential-step cyclic voltammetry in an attempt to elucidate the cation radical of p-phenylenediamine. The potential was held at + 0.60 Volts for 25 seconds and then cycled. The diagram reveals two oxidation peaks of which the first is assumed to indicate the cation radical before side reactions and dimerization occurs. This technique is highly qualitative with respect to stability and quantitative considerations. The technique however provides evidence for the successful generation of free radicals using electrochemical cell II.

Figures 29 and 30 are examples of chronoamperometric experiments. The main point to be considered here is the greater current decay of Figure 30. Spinning promotes greater efficiency.

Experiments were conducted in an attempt to coat mercury on the RVC working electrode to expand the potential window and cover the organic functional groups that may attach themselves to RVC and inhibit the reactions of aromatic compounds. The experiments were largely unsuccessful. There was large background noise that occurred during the entire cyclic voltammetry experiment. The noise was never reduced. The procedure was varied from the literature using as high as 30 parts per million of mercury in solution to obtain a smooth mercury coating. The electrode never equilibrated. It was concluded that platinum must first be plated on the RVC before attempting to deposit the mercury.
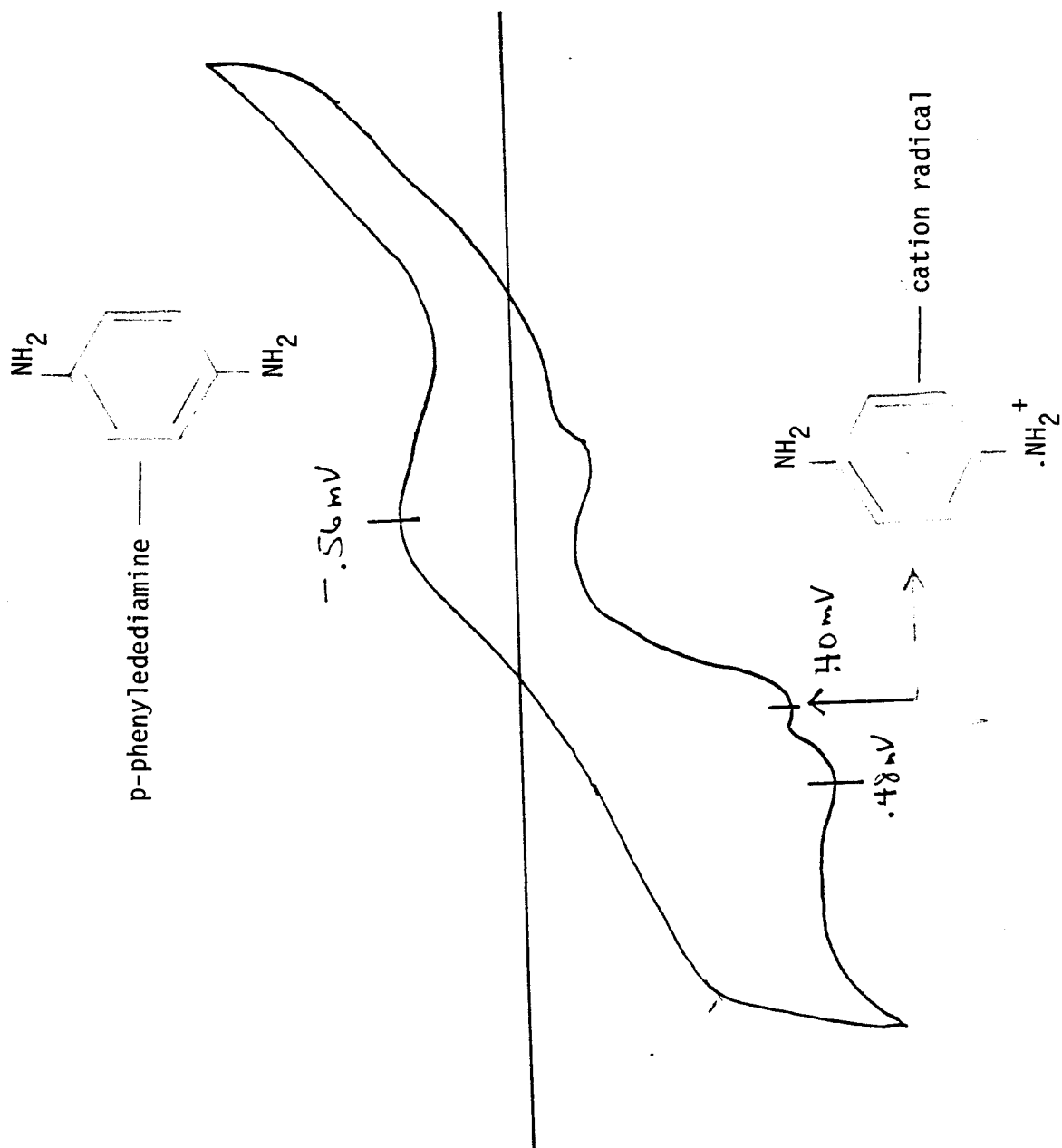
Figure 28: Potential step cyclic voltammetry of 25 mM p-phenyle-
nediamine in 1.0 M KCl. Resolution of the cation
radical is assumed at a potential of 0.40 volts.

Figure 29: Example of a chronoamperometric experiment with a
constant potential of 0.50 volts vs. Ag/AgCl applied
to 10 mM potassium ferrocyanide in 1.0 M KCl. The
current range is 10 mA with a sweep setting of 10
sec/cm. The cell is not spinning. Each large block
is one cm.

Current Key

1.0 Volt = 10mA full scale
1.0 mV = 10uA full scale
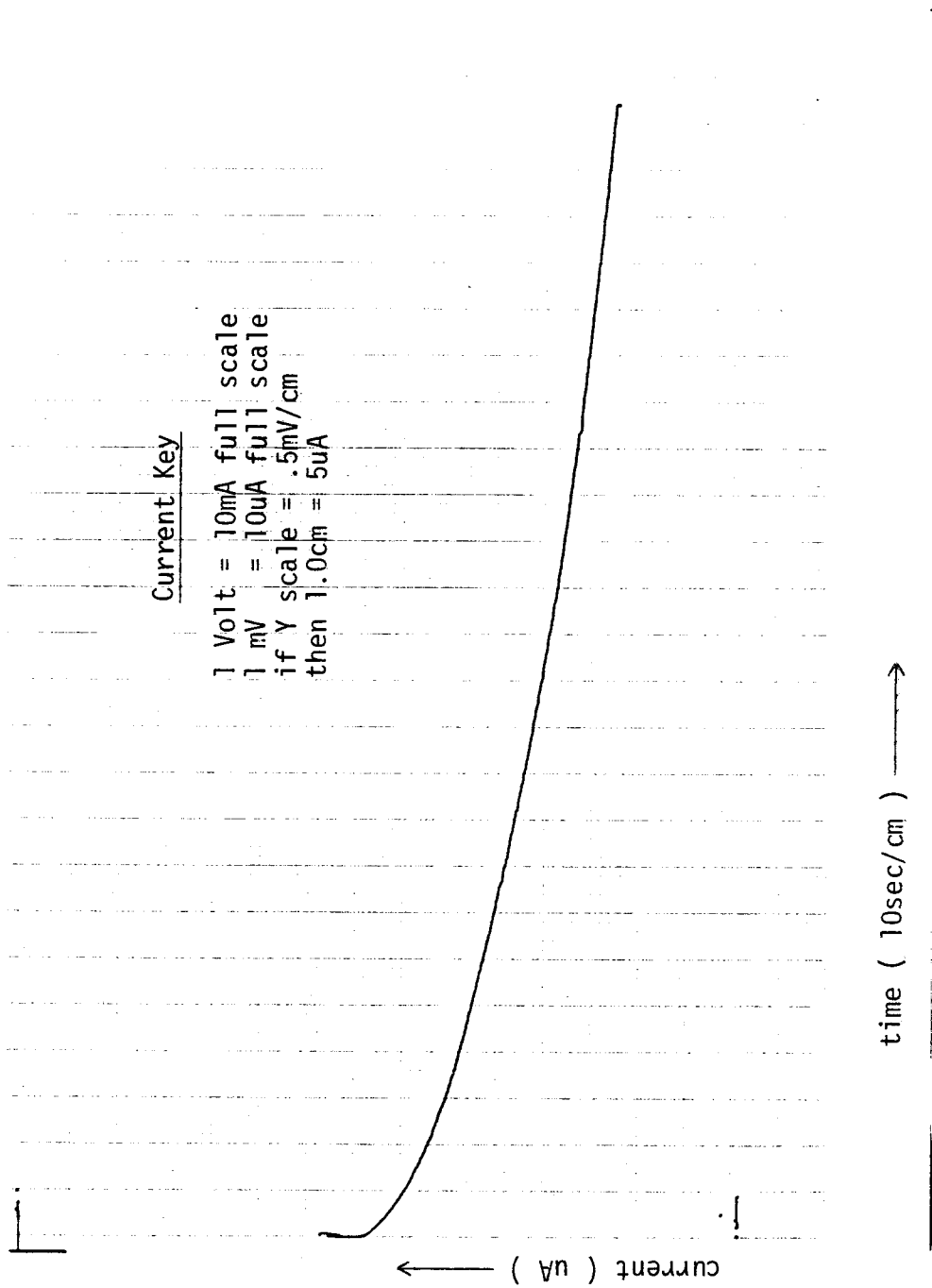if Y scale = .5mV/cm
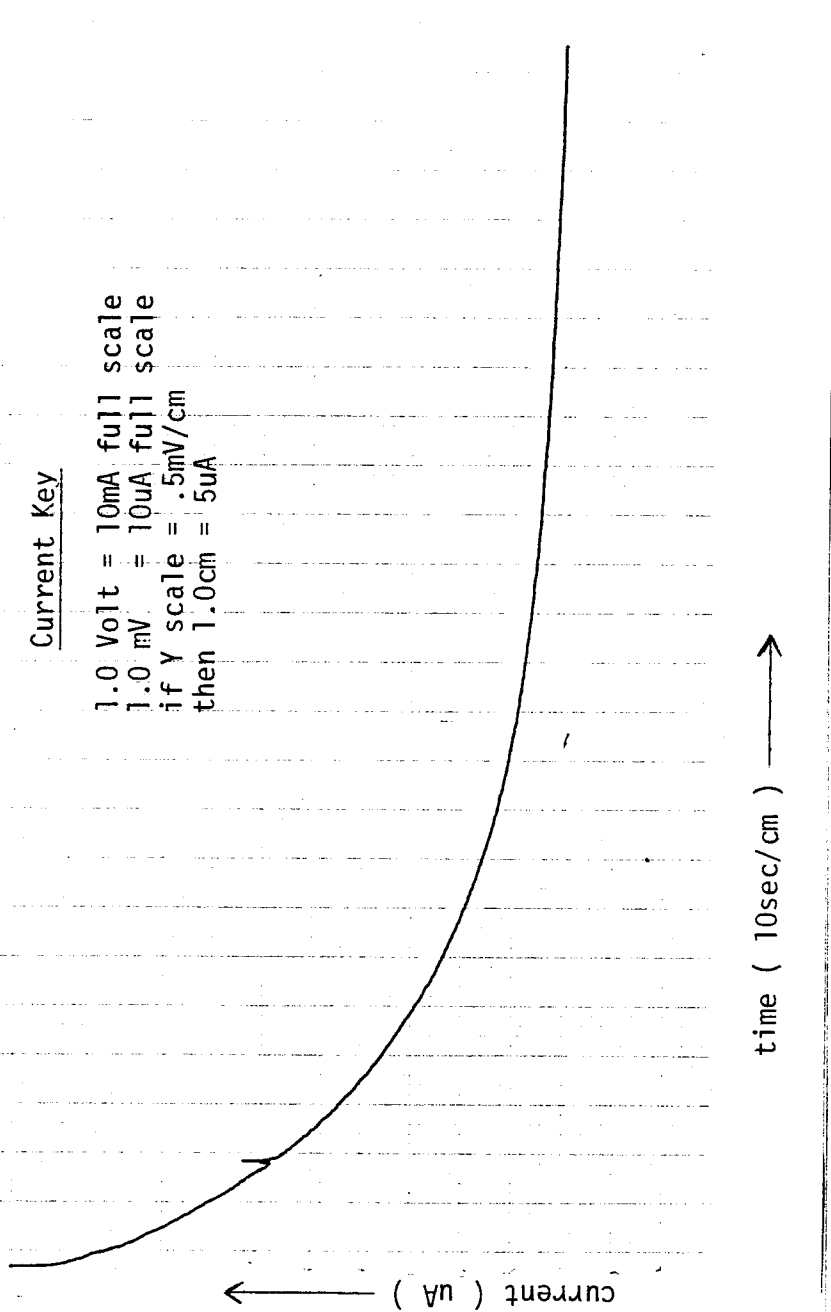then 1.0cm = 5uA

time (10sec/cm) ⟶

current (uA)

Figure 30: Example of a chronoampherometric experiment with a
constant potential of 0.5 volts applied to 10 mM
potassium ferrocyanide in 1.0 M KCl. The current
range is 10 mA with a sweep setting of 10 sec/cm.
The cell is spinning at 60 rpm. Note the current
decay with respect to Figure 29. Each large block
is one cm.

CHAPTER VI

CONCLUSION

From this investigation the following conclusions can be reached: (1) The design of electrochemical Cell II is satisfactory in that operation is reproducible over an extended period of time, and efficiency of operation that is necessary to electrolyze very small volumes of solutions of very low concentrations exist. (2) The work done in this investigation is believed to be the first successful regeneration of reticulated vitreous carbon for use beyond two weeks. This serves to indicate both the utility of RVC as an electrode material and the necessary benefit of consistently using the same electrode to determine proper cell operation over an extended period of time. (3) Free radicals can probably be produced using electrochemical cell II, but attempts to determine their concentration and stability were unsuccessful. Further work is necessary to investigate the stability of free radicals generated by an electrochemical cell that utilizes RVC electrodes, to determine if a great enough concentration is present to be detected in an NMR spectrometer.

Further work should involve not only quantitative cell design parameters, but also should attempt to use this technique to determine radical structural and kinetic information in an NMR spectrometer.

APPENDIX A

PROCEDURE FOR PREPARING AND MAINTAINING A Ag/AgCl REFERENCE ELECTRODE

The Ag/AgCl reference electrode was made by taking silver wire (28 gauge) and placing it into a 1 M solution of potassium chloride. The silver wire will become the working electrode in an electrochemical cell that has an SCE reference electrode and a platinum auxiliary electrode. An applied potential of + 0.40 Volts vs. SCE is provided for 2 or 3 minutes so that silver chloride is coated on the silver wire.

The silver wire that has been coated with silver chloride is then introduced into tube A, which has a 4 M solution of KCl saturated with silver ion. The 4 M solution of KCl is the standard solution utilized in Ag/AgCl reference electrodes. Any change of this salt concentration will cause a change in the reference potential. There is the need for the vycor plug at the bottom of tube A to isolate the internal and external solutions. Vycor allows contact between the external 1 M solution of KCl and the internal 4 M solution of KCl and saturated silver ion, but will minimize their mixing. Since diffusion across the vycor plug will still occur, it is necessary to replace the internal solution each morning. It is also necessary to remove any salt that builds up at the entrance to tube A.

When the silver wire that is coated with silver chloride is introduced into tube A, no air bubbles must be present around the electrode wire or tapped in the internal solution. This is especially true near the vycor plug, since this will create large shifts in the appropriate potential. The vycor plug must always remain wet or in contact with a 1 M KCl solution or it will dry out and lose its porocity to electrons.

During electrolysis the silver chloride that is deposited on the silver wire may go back into solution. It is necessary to redeposit chloride on the silver wire at least once a week.

APPENDIX B

PROCEDURE FOR THE REGENERATION OF RETICULATED VITREOUS CARBON

Once the RVC has been used for an experiment, it is necessary to use the following procedure to regenerate the electrode surface. The electrode is washed twice with deionized water. It is then washed with dilute nitric acid (HNO_3). It is allowed to sit in the HNO_3 for 3-5 minutes. The electrode is then washed with deionized water. It is then washed with 1.0 M KCl solution and is introduced into a new 1.0 M KCl solution and allowed to sit for 10 minutes.

The working electrode is then reconnected to the cell which has a fresh 1.0 M KCl solution and is cycled for 10-15 minutes between the potential limits of 1.2 Volts and -1.2 Volts at a scan rate of 2 mv/s. This must be done after each experiment beyond two weeks after the initial use of the material.

The consequences of not using the procedure for regeneration are indicated by potential lag as well as the presence of a large noise to signal ratio over the entire cycle. It should be noted that the cycling is done at slow scan rates of 5 mV/sec. After 10-15 minutes the equilibration will be complete and the electrode will be ready to use. This is indicated by the large noise to signal ratio that will eventually be resolved to a standard response or a clean cyclic voltammogram. If this does not completely eliminate the noise, it is necessary to allow the

electrode to stand for 24 hours in a fresh 1.0 M KCl solution and
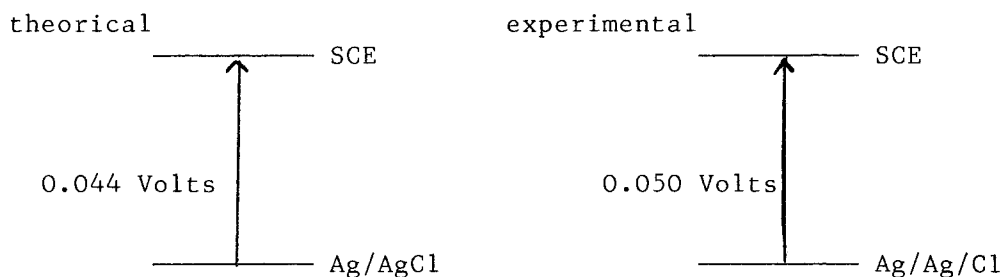
begin the cycling procedure again.

APPENDIX C

ELECTRODE CONVECTION

Electrochemical measurements require that the half-cell potential of one of the electrodes be known. It is not possible to measure the potential of one of the electrodes without first connecting the electrode to a potential measuring device. This would mean introducing the device into the solution to create electrical contact. This contact will involve a second solid-solution interface and will act as another electrode, or a second half-cell at which a chemical reaction must occur if current is to flow. A potential will be the result of this second reaction. This potential will be measured and results in a general inability to obtain an absolute potential measurement for a half-cell or electrode.

If we choose an electrode to have an arbitrary value of zero potential, then we can reference our electrode against this electrode to determine the potential. The convention for referencing electrode potentials to a primary reference electrode such as a standard hydrogen electrode (NHE), are given here.

The Ag/AgCl reference electrode that was used in electrochemical cell II was referenced against the SCE. The experimental value was 0.050 Volts vs. a theorical value of 0.044 Volts. This indicates

the Ag/AgCl reference electrode is operating properly. This can be shown as,

```
      theorical                        experimental
   _____ ↑ ___ SCE           _____ ↑ ___ SCE

  0.044 Volts │                   0.050 Volts │

   _____ │ ___ Ag/AgCl        _____ │ ___ Ag/Ag/Cl
```

To determine the proper redox potentials that are reported by the literature, consideration of electrode convention is appropriate and necessary. The literature reports values for the oxidation of potassium ferrocyanice to be 0.328 Volts and 0.336 Volts vs. an SCE. Since this investigation used a Ag/AgCl reference electrode, it is necessary to convert the literature values reported vs. an SCE to appropriate values vs. a Ag/AgCl. This can be shown as,

```
      experimental 1                    experimental 2

 0.372 Volts  ↑   ↑                0.380 volts  ↑   ↑
              │   │ 0.328 Volts                 │   │ 0.336 Volts
   _____│___│___ SCE           _____│___│___ SCE
              ↑ 0.044 Volts                     ↑ 0.044 Volts
   _____↓_____ Ag/AgCl        _____↓_____ Ag/AgCl
```
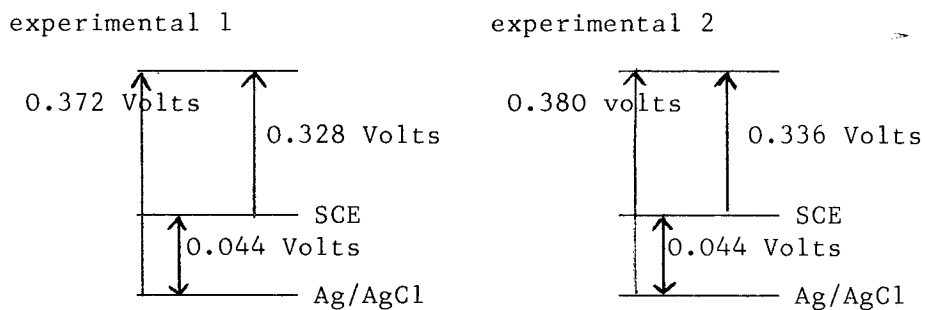
The experimental value of 0.37 Volts experimentally determined during this investigation can now be compared to the above experimental literature values.

REFERENCES

1. Pryor, W. A., *Sci. Amer.* 1970, 223, 70.

2. Kuwana, T., Darlington, R. K., and Leedy, D. W., *Anal. Chem.* 1964, 36, 2023.

3. Heineman, W. R., *Anal. Chem.* 1978, 50, 390A.

4. Tallant, D. R., and Evans, D., *Anal. Chem.* 1969, 41, 835.

5. Kissinger, P. T., and Reilly, C. N., *Anal. Chem.* 1970, 42, 12.

6. Mark, H. B., and Pons, B. S., *Anal. Chem.* 1975, 47, 736.

7. Jean, D. L., Suchanski, M. R., and Van Duyne, R. P., *J. Am. Chem. Soc.* 1975, 97, 1699.

8. Hawkridge, F. M., and Ke, B., *Anal. Biochem.* 1977, 78, 76.

9. McIntyre, J. D. E., "New Spectroscopic Methods for Electrochemical Research," in *Trends in Electrochemistry*, Edited by Bockris, J. O'M., Rand, D. A. J., and Welch, B. J. New York: Plenum Press, 1977.

10. Richard, J. A., and Evans, D., *Anal. Chem.* 1975, 47, 964.

11. Mincey, D. W., Popovich, J. J., Faustino, P. J., Caruso, J. A., and Hurst, M. M., *Anal. Chem.* in press.

12. McKinney, T. M., "Electron Spin Resonance in Electrochemistry" in *Electroanalytical Chemistry*, Vol. 10 Edited by Bard, A. J. New York: Marcel Dekker, 1977.

13. Leyden, D. E., and Cox, R. H., *Analytical Applications of NMR*. New York: Academic Press, 1977.

14. Farrar, T. C. and Becker, E. D., *Pulse and Fourier Transform NMR*. New York: Academic Press, 1971.

15. James, T. L., *Nuclear Magnetic Resonance Spectroscopy in Biochemistry*. New York: Academic Press, 1975.

16. Bovey, F. A., *Nuclear Magnetic Resonance Spectroscopy*. New York: Academic Press, 1969.

17. Ionin, B. I., and Ershov, B. A., *NMR Spectroscopy in Organic Chemistry*. New York: Plenum Press, 1970.

18. Brokris, J. O'M., and Reddy, A. K. N., Modern Electrochemistry. New York: Plenum Press, 1970.

19. Fried, I., The Chemistry of Electrode Processes. London: Academic Press, 1973.

20. Bockris, J. O'M., and Drazic, D. M., Electrochemical Science. London: Taylor & Francis Ltd., 1972.

21. Bockris, J. O'M., Bonciocat, N., and Gutman, F., An Introduction to Electrochemical Science. London: Wykeham Publications Ltd., 1974.

22. Ref. 18, p. 752.

23. Conway, B. E., Theory and Principles of Electrode Processes. New York: The Ronald Press Company, 1965.

24. Stern, O., Z. Electrochem. 1924, 30, 508.

25. Ref. 18, p. 736.

26. Ref. 21, p. 57.

27. Bard, A. J., and Faulkner, L. R., Electrochemical Methods. New York: John Wiley & Sons, Inc., 1980.

28. Erdey-Gruz, T. Kinetics of Electrode Processes. New York: John Wiley & Sons, Inc., 1972.

29. Adams, R. N., Electrochemistry at Solid Electrodes. New York: Marcel Dekker, 1969.

30. Lingane, J. J., Electroanalytical Chemistry. New York: Interscience Publishers, Inc., 1958.

31. Harrar, J. E., and Shain, I., Anal. Chem. 1966, 38, 1148.

32. Booman, G. L., and Holbrook, W. B., Anal. Chem. 1965, 37, 795.

33. Harrar, J. E., and Pomernacki, C. L., Anal. Chem. 1973, 45, 47.

34. Britz, D., J. Electroanal. Chem. 1978, 88, 309.

35. Sawyer, D. T., and Roberts, J. L., Experimental Electrochemistry for Chemists. Toronto: John Wiley & Sons, Inc., 1974.

36. Baizer, M. M., Organic Electrochemistry. New York: Marcel Dekker, 1973.

37. Harrar, J. E., and Shain, I., Anal. Chem. 1966, 38, 1157.

38. Eberson, L., and Schafer, H., *Organic Electrochemistry*. New York: Springer-Verlag, 1971.

39. Nicholson, R. S., and Shain, I., *Anal. Chem.* 1964, 36, 706.

40. Dohrman, J. K., and Vetter, K. J., *J. Electroanal. Chem.* 1969, 20, 23.

41. Korshonov, I. A., Kuznetsova, Z. B., and Shchennikova, M. K., *Chem. Abs.* 1950, 44, 2873.

42. Richards, J. A., Ph.D. Thesis, University of Wisconsin, 1975.

43. Ref. 29, p. 219.

44. Papouchado, L., Bacon, J., and Adams, R. N., *J. Electroanal. Chem.* 1970, 24, App. 1.

45. Peterson, W. M., and Wong, R. N., *Amer. Lab.* Nov. 1981, 116.

46. Blaedel, W. J., and Wang, J., *Anal. Chem.* 1980, 52, 1697.

47. Ref. 35, p. 77.

48. Ref. 29, p. 71.

49. Karp, S., and Meites, L., *J. Am. Chem. Soc.* 1962, 84, 906.

50. Bard, A. J., *Anal. Chem.* 1963, 35, 1125.

51. Norvell, V. E., and Mamantov, G., *Anal. Chem.* 1977, 49, 1470.

52. Sleszynski, N., Osteryoung, J. and Carter, M., *Anal. Chem.* 1984, 56, 130.

53. Calasanzio, D., Sorano, C., Zamponi, S., and Marassi, R., *Annali de Chimica.* 1983, 73, 161.